약학박사학위논문

지느러미 엉겅퀴와 캐모마일의 생리활성 물질에 대한 탐색적 분리

Bioactive principles from *Carduus crispus* and *Matricaria recutita* L. with anti-adipogenic and anti-inflammatory activities

2016년 8월

서울대학교 대학원

약학과 천연물과학전공

홍 유 나

ABSTRACT

Thistles, belonging to the Asteraceae, are too varied for generalization; many are troublesome weeds, including some invasive species of *Cirsium*, *Carduus*, *Silybum*, and *Onopordum*. *Carduus crispus*, native to Europe and Asia, is a traditional herbal medicine used for treating inflammatory disorders in Korea. Obesity is characterized by a state of chronic inflammation with increased inflammatory markers along with the expression and release of inflammation-related adipokines. Most anti-obesity drugs have been developed based on this concept. This research for anti-obesity agents derived from *Carduus crispus* utilized the 3T3-L1 cell line. The methanol extract was initially screened and exhibited significant inhibition of adipogenesis in 3T3-L1 adipocytes. Among five liquid-liquid partition fractions, the ethyl acetate (EA) fraction showed the most potent suppressive effect compared with hexane, chloroform, n-butanol, and water. The EA fraction was considered for further study because of the presence of abundant polyphenols, including flavonoids. To isolate the active components from the EA fraction, elution-extrusion counter-current chromatography (EECCC) was used. Among the seven fractions from the EA layer, fraction 6 inhibited lipid accumulation as well as CCAAT/enhancer-binding protein alpha (C/EBPα) and peroxisome proliferator-activated receptor gamma (PPARγ) protein expression levels. The

active component apigenin (fraction 6) was confirmed using high-performance liquid chromatography (HPLC), electrospray ionization mass spectrometry (ESI-MS), and one-dimensional nuclear magnetic resonance (1D-NMR) spectroscopy. The present data suggest that apigenin is one of the main bioactive compounds from *Carduus crispus* for inhibiting adipogenesis in 3T3-L1 adipocytes via the activation of AMP-activated protein kinase. Using the marker substance pectolinarin, isolated from *Cirsium japonicum*, one of the representative type of thistles, a dose-dependent decrease on lipid accumulation was identified in 3T3-L1 adipocytes. This inhibitory effect on adipogenesis was shown to be induced by the suppression of a sterol regulatory element binding protein-1 (SREBP-1) and the activation of adenosine monophosphate-activated protein kinase (AMPK). The findings that the generation of intracellular reactive oxygen species (ROS) and the expression of heme oxygenase-1 (HO-1) proteins were inhibited suggest that this anti-adipogenic effect resulted from lipid oxidation. The present study demonstrates that apigenin from *Carduus crispus* and pectolinarin from *Cirsium japonicum* have reduced the lipid accumulation with their significantly inhibition of PPARγ and C/EBPα protein expressions and the activation of AMPK. However, apigenin exhibited cytotoxicity at 50 μM not in pre-adipocytes but in mature adipocytes and pectolinarin has no cytotoxic effect on both types of cells. In summary, this study shows that apigenin has

shown the apoptotic 3T3-L1 cell death via the activation of AMPK and caspase-3. Whereas pectolinarin, against apigenin, has shown the lipid oxidation via the inhibition of intracellular ROS and HO-1 generation. Another member of Asteraceae, *Matricaria recutita* L. (chamomile) was also studied for the anti-inflammatory activity and bioactivity-guided isolation to search the active component. The inhibition effects of nitric oxide (NO) production and NF-κB secretory alkaline phosphatase (SEAP) activity of chamomile methanol extract exhibited better than those of water and ethanol extracts. Because methanol is less polar than water, the methanol extract contains more essential oils than the water extract. To identify the main volatile constituents of the essential oil in chamomile, dried chamomile powders were extracted by head space-solid-phase micro extraction (HS-SPME) and were analyzed by gas chromatography-mass spectrometry (GC-MS). Parameters affecting the solid-phase micro extraction (SPME) procedure including extraction temperature and time, amount of the sample, and desorption time have been evaluated and optimized. In addition, methanol and water extracts of chamomile, and hexane fractionation from the methanol extract of chamomile were analyzed to compare. A total of 41 components were identified. It is well known the principal biologically active compounds in chamomile oils were bisabolol oxide A, bisabolol oxide B, α-bisabolol, chamazulene, spathulenol, and β-farnesene. The powderized sample of dried

chamomile was rich in bisabolol oxide B (21.0 %), β-farnesene (17.9 %), and α-bisabolol (9.0 %). Herniarin (10.1 %) was predominant in the water extract. In case of the methanol extract and hexane layer, bisabolol oxide B (each of 21.7 %) was the most abundant component. α-bisabolol was detected only in dried chamomile powder. The compounds identified in the hexane layer fractionated from the methanol extract were found to be very similar to the volatile essential oils identified in the methanol extract. Based on the identification of essential oil components, the organic solvent extracts containing large amounts of essential oil components are thought to have a higher anti-inflammatory effect. Therefore, the non-volatile compound of methanol extract from chamomile was also analyzed to identify anti-inflammatory compounds. Fractionation using liquid-liquid separation was performed to identify non-volatile active compounds as well. The methanol extract of chamomile was fractionated into hexane, EA, BuOH, and water layers. The less polar hexane and EA-soluble layers were shown, as expected, to have higher inhibitory effects on NO generation and NF-κB expression, but the hexane-soluble layer was also found to have cytotoxicity. Therefore, the EA-soluble layer containing large amount of flavonoids was selected for further separation. The EA-soluble layer was separated into seven fractions by silica gel column chromatography. Of those seven fractions, 5th fraction with no toxicity and high yield was selected to be further separated. In the next step,

5th fraction was separated into a total of 5 fractions using Diaion HP-20 column chromatography. From those fractions, 3 main components - dicaffeoyl quinic acids enriched (50% MeOH, DCQ), apigenin 7-O-glucoside derivatives enriched (70% MeOH, A7G) and tetracoumaroyl thermospermine enriched (90% MeOH, TCTS) – were identified, among which TCTS was shown to have the highest NO inhibition effect. Within the range of concentrations at which no cytotoxicity was observed, TCTS was assayed for the expression of proteins associated with inflammation using Western blot analysis. TCTS was shown to have higher inhibitory effects on the expressions of inducible nitric oxide synthase (iNOS) and cyclooxygenase-2 (COX-2) compared to those of DCQ and A7G and, in particular, was found to inhibit COX-2 selectively without affecting cyclooxygenase-1 (COX-1) expression. In this study, it was also found that the inhibition of COX-2 of TCTS was exerted via extracellular signal-regulated kinases (ERK)/Akt and signal transducer and activator of transcription 3 (STAT3) pathway. The purpose of this study included the identification of essential oil components and the bioactivity-guided isolation for non-volatile active compounds responsible for chamomile's anti-inflammatory effect. The result showed that the dried German chamomile contained large amounts of anti-inflammatory volatile compounds such as α-bisabolol oxide B, β-farnesene and α-bisabolol. The higher anti-inflammatory effect shown in the methanol extract than in the

water extract was deemed to be due to the greater amount of essential oil components, in particularly α-bisabolol oxide B, contained in the methanol extract. The bioactivity-guided isolation performed to explore non-volatile active components showed that TCTS is mainly responsible for the anti-inflammatory effect of chamomile with COX-2 inhibition via ERK/Akt and STAT3 pathway.

Keyword : *Carduus crispus*, apigenine, pectolinarin, chamomile, tetracoumaroyl thermospermine, anti-adipogenesis, anti-imflammation

Student Number : 2009-30474

Table of Contents

ABSTRACT 1

Table of Contents 7

List of Figures 13

List of Tables 15

CHAPTER I. Anti-adipogenic activity of *Carduus crispus* in mature adipocyte and bioactivity-guided isolation of its active component compared to the activity of pectolinarin from *Cirsium japonicum* 16

1. Introduction 17

1.1. Adipogenesis 17

1.1.1. Obesity 17

1.1.2. Adipocyte differentiation 18

1.2. Thistles: *Carduus crispus* L. and *Cirsium japonicum* 20

1.3. High-speed counter-current chromatography 21

2. MATERIALS AND METHODS 26

2.1. Materials 26

2.1.1. Chemicals and reagents 26

2.1.2. Sample preparation 27

2.1.3. Apparatus 29

2.2. Methods 30
2.2.1. Cell culture 30
2.2.2. Cell viability assay 30
2.2.3. Oil Red O staining..... 31
2.2.4. Intracellular ROS..... 31
2.2.5. Western blot analysis..... 32
2.2.6. Statistical analysis 33
3. Results.....34
3.1. Inhibitory effect of the *Carduus crispus* methanol extract on lipid accumulation in 3T3-L1 Cells.....34
3.2. Effects of the five liquid layers from *Carduus crispus* methanol extract on the expression of PPARγ and C/EBPα proteins in 3T3-L1 cells 37
3.3. Selection of the two-phase solvent system on EECCC.....40
3.4. Structural identification.....44
3.5. Effects of the EECCC fractions from the EA-soluble layer of *Carduus crispus* on lipid accumulation in 3T3-L1 cells 45
3.6. Effects of apigenin on the cell viability and accumulation of lipid droplets in 3T3-L1 cells 47
3.7. Effects of apigenin from the EA layer of *Carduus crispus* on the expression of proteins associated with differentiation

induction.....47
3.8. Effects of pectolinarin from *Cirsium japonicum* on lipid accumulation in 3T3-L1 cells.....52
3.9. Effects of pectolinarin from *Cirsium japonicum* on intracellular ROS generation in 3T3-L1 cells 52
3.10. Effects of pectolinarin from *Cirsium japonicum* on the Expression of Proteins Associated with Differentiation Induction.....52
4. Discussion.....57
CHAPTER II. Optimization of headspace-solid phase micro extraction coupled to gas chromatography mass spectrometer for the chemical composition analysis of chamomile (*Matricaria recutita* L.) and bioactivity-guided isolation of its anti-inflammatory active components.....61
1. Introduction 62
1.1. Inflammation 62
1.2. *Matricaria recutita* L.....63
1.2.1. German chamomile 63
1.2.2. Essential oils..... 65
1.3. HS-SPME/GC-MS 66
2. MATERIALS AND METHODS 72

2.1. Materials 72
2.1.1. Chemicals and reagents 72
2.1.2. Sample preparation 73
2.1.3. Apparatus 75
2.2. Methods 75
2.2.1. HS-SPME extraction 75
2.2.2. GC-MS analysis 76
2.2.3. Primary cell culture 77
2.2.4. Cytotoxicity assay 77
2.2.5. Assay for nitrite inhibition effect 77
2.2.6. NF-κB SEAP reporter gene assay 78
2.2.7. Western blot analysis 79
2.2.8. Statistical analysis 79
3. Results 81
3.1. Optimization of HS-SPME coupled to GC-MS for the chemical composition analysis of chamomile (*Matricaria recutita* L.) 81
3.1.1. Extraction profile obtained with different sample amount for six major compounds 81
3.1.2. Extraction profile obtained with different extraction time for six major compounds 81

3.1.3. Extraction profile obtained with different extraction temperature for six major compounds 82
3.1.4. Extraction profile obtained with different desorption time for six active compounds 82
3.1.5. SPME/GC-MS identification of chamomile volatiles and peak area percentage 86
3.1.6. Comparison of the different extract composition obtained by SPME/GC-MS 90
3.2. Bioactivity-guided isolation of anti-inflammatory active component from chamomile methanol extract 94
3.2.1. Inhibition of chamomile water, ethanol and methanol extract on cell viability, LPS-induced NO production and NF-κB SEAP activity 94
3.2.2. Inhibition of its liquid layers from chamomile methanol extract on cell viability, LPS-induced NO production and NF-κB SEAP activity 97
3.2.3. Inhibition of fractions isolated by silica gel column chromatography from chamomile EA extract on cell viability and LPS-induced NO production and NF-κB SEAP activity 99
3.2.4. Inhibition of three enriched fractions isolated by Diaion HP-20 chromatography from 5th fraction by silica gel chromatography on

cell viability and LPS-induced NO production 101

3.2.5. Inhibition of three enriched fractions isolated by Diaion HP-20 chromatography from 5th fraction by silica gel chromatography on the protein levels of COX-1, COX-2, and iNOS in LPS stimulated RAW 264.7 macrophages 103

3.2.6. Inhibition of tetra-coumaroyl thermospermine enriched fractions on the protein levels of ERK, Akt, and STAT3 in LPS stimulated RAW 264.7 macrophages 106

4. Discussion 108

5. References 113

ABSTRACT IN KOREAN 123

List of Figures

Figure 1. Adipocyte life cycle 23

Figure 2. *Carduus crispus* 24

Figure 3. Roadmap of extraction and separation by HSCCC..... 25

Figure 4. Schematic of the extraction and separation of the *Carduus crispus* extract. 28

Figure 5. Inhibitory effects of the *Carduus crispus* methanol extract on lipid accumulation and PPARγ and C/EBPα protein expression during adipogenesis. 36

Figure 6. Inhibitory effects of different fractions from *Carduus crispus* on PPARγ and C/EBPα protein expression during adipogenesis. 38

Figure 7. The HSCCC chromatograms of the EA extract from *Carduus crispus*. 41

Figure 8. Inhibitory effects of apigenin extracted from *Carduus crispus* on lipid accumulation and induction of differentiation and apoptosis in 3T3-L1 mature adipocytes. 50

Figure 9. Inhibitory effects of pectolinarin extracted from *Cirsium japonicum* on lipid accumulation and induction of lipid oxidation in 3T3-L1 adipocyte cells. 56

Figure 10. Chamomile (*Matricaria recutita* L.) 68

Figure 11. HS-SPME system..... 69

Figure 12. Chemical structures of major ingredients of chamomile 71

Figure 13. Schematic of the extraction and separation of German chamomile (*Matricaria recutita* L.) 74

Figure 14. Extraction profile obtained with different analysis conditions for six active compounds in dried chamomile. 85

Figure 15. Effect on NO and NF-κB inhibition of various extracts from chamomile 96

Figure 16. Effect on cell viability, NO production and NF-κB SEAP activity of different fractions from chamomile methanol extract..... 98

Figure 17. Effect on cell viability and NO production of different fractions from chamomile EA extract 100

Figure 18. Effect on cell viability and NO production of different fractions from chamomile EA extract 102

Figure 19. Effect of three enriched fractions from chamomile on the protein levels of iNOS, COX-1, and COX-2 in LPS-induced RAW 264.7 macrophages..... 104

Figure 20. Effect of TCTS on the ERK, Akt, and STAT3 pathways 107

List of Tables

Table 1. Partition coefficient (*K*) values of *Carduus crispus* in different solvent systems. 42

Table 2. Inhibitory effects of each fraction from EECCC on lipid accumulation in 3T3-L1 adipocytes. 46

Table 3. Essential oil components extracted by HS-SPME from dried chamomile at GC-MS 87

Table 4. Essential oil components extracted by HS-SPME from water extract, methanol extract and hexane layer from chamomile methanol extract at GC-MS 92

CHAPTER I.

Anti-adipogenic activity of *Carduus crispus* in mature adipocyte and bioactivity-guided isolation of its active component compared to the activity of pectolinarin from *Cirsium japonicum*

CHAPTER I.

Anti-adipogenic activity of *Carduus crispus* in mature adipocyte and bioactivity-guided isolation of its active component compared to the activity of pectolinarin from *Cirsium japonicum*

1. Introduction

1.1. Adipogenesis

1.1.1. Obesity

Excessive body fat is accompanied by serious public health problems [1]. Obesity is associated with not only psychological problems involving an inferiority complex but also serious metabolic diseases such as fatty liver, type II diabetes mellitus, cardiovascular disease and cancer [2-4]. To prevent these serious problems, anti-obesity drugs, which function by either reducing appetite or inhibiting fat absorption, are used [5]. There are four key methods to block fat generation: 1) inhibition of cell proliferation on preadipocyte development, 2) inhibition of differentiation and lipid accumulation at the stage of maturing adipocytes, 3) lipolysis and 4) acceleration of apoptosis in mature adipocytes (Figure 1)[6]. However, current pharmacological medications such as orlistat and sibutramine appear to have limited efficacy and hazardous side-effects, including increased blood pressure, dry mouth, constipation, headache and insomnia [7-10]. Therefore, it is necessary to develop new agents from effective and safe natural plants to treat obesity and overweight. Several plants, such as ginseng, gingko, Echinacea, garlic, chamomile and fruits, have been verified as medicinally beneficial through repeated clinical testing and laboratory analysis [11] and a number of plant extracts such as green tea [12], garlic compounds [13] and conjugated linoleic

acid (CLA) [14] have been shown to possess either anti-diabetic effects or have direct effects on adipose tissue. Many bioactive components from nature are potentially useful in obesity treatments, with polyphenols as a good example. These show strong anti-obesity activity and include apigenin, genistein and the catechins [15-17].

1.1.2. Adipocyte differentiation

3T3-L1 cells are widely used in basic research of adipocytes and in pharmaceutical studies and an appropriate preadipocyte in vitro model for studying differentiation and obesity metabolism, because adipocyte differentiation plays an important role during the induction of obesity [18, 19]. Efficient differentiation of 3T3-L1 cells into mature adipocytes containing lipid droplets was confirmed when the cells were treated with differentiation inducers such as 3-isobutyl-1-methylxanthine (IBMX), dexamethasone and insulin; the differentiation was accompanied by an increase in adiponectin release[20, 21]. One of the multifactorial causes for obesity is unregulated genes, such as the PPARγ and C/EBPα which stimulates lipid metabolism [22]. PPARγ and C/EBPα are important major transcription factors, known as a key station protein in the adipocyte differentiation of 3T3-L1 cells [23].

AMPK is a serine/threonine protein kinases, which is activated by cellular stresses that deplete adenosine triphosphate (ATP) [24]. Identification

of physiological processes in which the enzyme plays a crucial role indicates the control of body fat stores by AMPK [25, 26]. In principle, there are two pathways to diminish adipose tissue mass: one is by a reduction of adipocyte volume, and the other, by reduction of adipocyte number [27, 28]. The decrease of the adipose tissue mass is usually attributed to loss of stored lipids by lipolysis rather than through fat cell loss. Yet, attempts to attribute to AMPK a role in the lipolytic process have yielded contradictory results. While Yin et al. demonstrated the essential role of AMPK in lipolysis, others have claimed the opposite – that AMPK activity is anti-lypolytic [29, 30]. Decrease of adipose tissue in human cell could result from loss of fat cells through programmed cell death [31, 32]. Following hormonal and metabolic stimulators of peripheral AMPK such as leptin and severe nutrient deprivation can mediate fat mass depletion through apoptotic pathways [33, 34].

ROS are produced by adipocytes during adipogenesis. ROS status in the cell modulates cellular physiology including growth and proliferation by affecting signaling molecules [35]. Recent studies have shown that ROS generation is associated with the pathogenesis and development of metabolic diseases as shown by the increased prevalence of obesity and diabetes [36, 37]. In particular, increased ROS production in adipose tissue of obese mice has been in company with activation of nicotinamide adenine dinucleotide phosphate hydrogen (NADPH) oxidase and inhibition of antioxidant enzymes

[36].

1.2. Thistles: *Carduus crispus* L. and *Cirsium japonicum*

Thistles are all members of the Asteraceae family, Cynareae strain and have been identified about two hundred fifty species around the world. Among them, about ten species have been found in Korea.

Carduus crispus L., commonly known as welted thistle, has been used as a traditional herbal medicine in Korea to cure different types of inflammation, such as arthritis, hemostasis and fever. Extracts from this plant have been found to have anti-cancer properties, with the main component being crispine A [38]. It was reported that among the seven Korean thistles, *Carduus crispus,* composed of luteolin and apigenin derivatives, has shown the strongest antioxidant capacity [39]. A previous study has demonstrated that the *Carduus crispus* methanol extract inhibited adipocyte differentiation through ERK and p38 mitogen-activated protein kinases (MAPK) pathways [40].

Cirsium japonicum, the milk thistle, is one of the most popular herbal remedies used by patients with liver disease [41]. It has been prescribed for the treatment of tumors, such as liver cancer, uterine cancer and leukemia, anti-hemorrhagic and diuretic agent in folk medicine. Recent studies have been reported that *Cirsium japonicum* flavones exert antimicrobial, antitumor

and antioxidant effects [39, 42]. Flavonoid compounds are the major chemical content in *Cirsium japonicum*. In particularly, pectolinarin is the primary component of *Cirsium japonicum*.

1.3. High-speed counter-current chromatography

In recent years, as an advanced separation technique, high speed counter-current chromatography (HSCCC) has been widely used to isolate active components from traditional herbal medicines and other natural products. This instrument was first invented by Ito [43]. HSCCC instruments are a modern and popular type of countercurrent chromatography (CCC) apparatus. In contrast to centrifugal partition chromatography (CPC), there are no rotating seals. Most modern HSCCC instruments contain multiple (usually two or three) separation coils. Compared to the conventional column chromatography, HSCCC is a kind of support-free all-liquid partition chromatographic technology, which eliminates the irreversible adsorption of the sample onto solid support and has an excellent sample recovery. What is more, it has a large amount of sample injection: multiform relative pure substances can be obtained at one time in large amount. It is gaining increasing interest recently, and is used more and more frequently in the isolation and purification of bioactive components from crude materials of various natural products. A literature investigation revealed that HSCCC

equipment is always coupled with an ultraviolet (UV) detection, which is of benefit to the isolation of the components with UV absorptions including flavonoids, coumarins, lignans etc., while the isolation of the components without UV absorption using HSCCC are very sparse. In the previous investigation, many active components from crude materials have been successfully isolated by HSCCC coupled an UV detection [44-49]. Herein, we reported a successful method to isolate active compound from the *Carduus crispus* L. using HSCCC coupled with evaporative light scattering detector (ELSD). For the high recovery and the high efficiency, this method has been met with increasing popularity for the preparative separation of natural products in recent years.

The purpose of this study is to determine which components from *Carduus crispus* L. have potent activity against adipogenesis in mature 3T3-L1 cells not pre-adipocyte and the mechanism of these components. In addition, comparative study was performed the marker substance pectolinarin, isolated from *Cirsium japonicum,* one of the representative type of thistles on anti-adipogenesis activity.

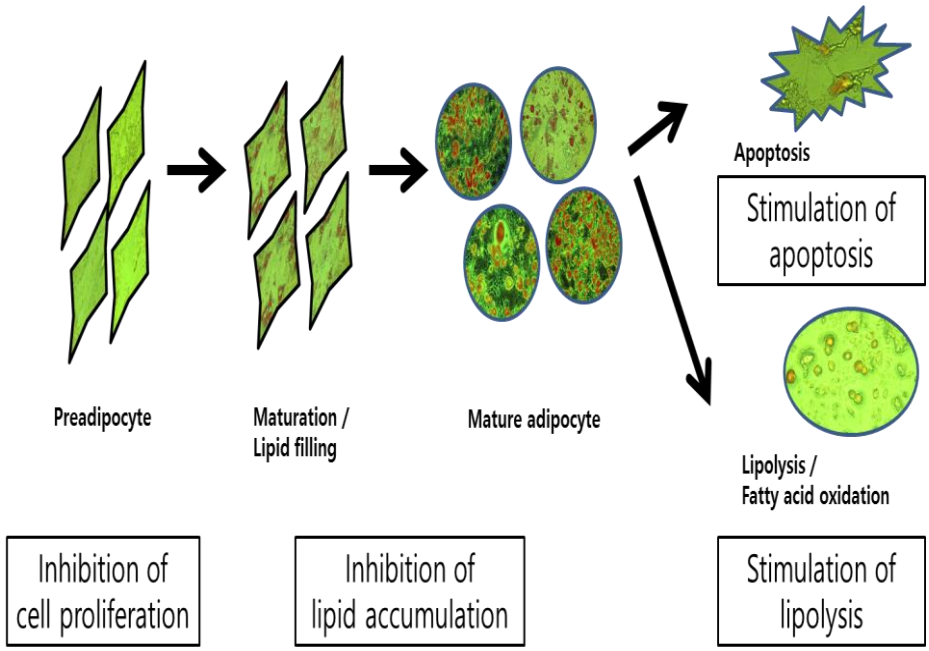

Figure 1. Adipocyte life cycle

Figure 2. ***Carduus crispus***

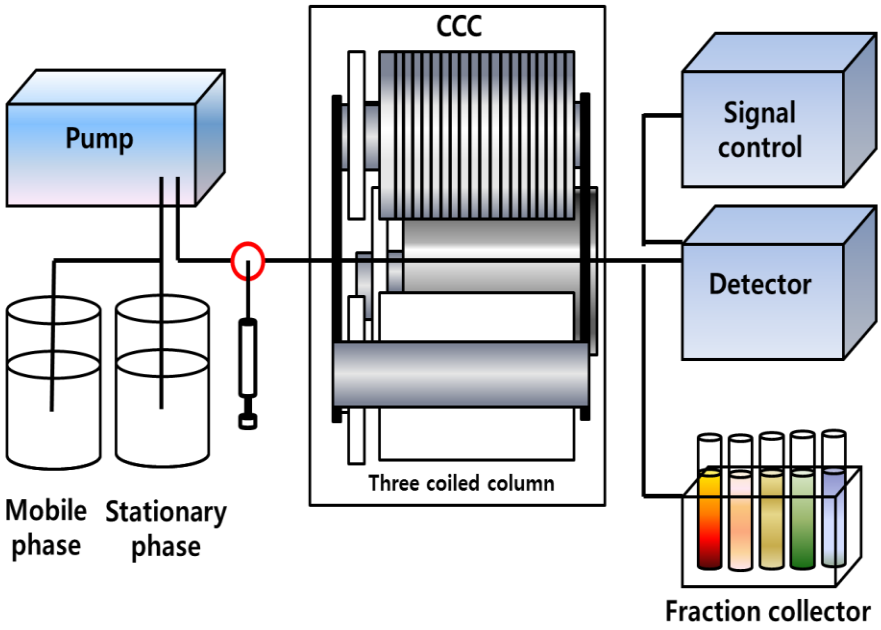

Figure 3. Roadmap of extraction and separation by HSCCC

2. MATERIALS AND METHODS

2.1. Materials

2.1.1. Chemicals and reagents

Pectolinarin (purity > 99.8%) was kindly provided by Professor Jae-soo Choi of Bukyoung University.

Dulbecco's modified Eagle medium with L-glutamine (DMEM) and 4-(2-hydroxyethyl)-1-piperazineethane-sulfonic acid (HEPES) were purchased from Gendepot (Barker, TX). Dulbecco's phosphate-buffered saline (D-PBS), 3-[4,5-dimethylthiazol-2-yl]-2,5-diphenyltetrazolium bromide (MTT), sodium bicarbonate, naphtylethylenediamine dihydrochloride, and other reagents not mentioned were purchased from Sigma Chemical Co. (St. Louis, MO). Penicillin-streptomycin, trypsin, ethylenediaminetetraacetic acid (EDTA), trypan blue, recombinant human insulin, IBMX, dexamethasone, Oil Red O, and NP-40 were purchased from Sigma-Aldrich (St. Louis, MO). Dimethyl sulfoxide (DMSO) (Bioshop, Burlington, Canada), fetal bovine serum (FBS) (South Pacific, New Zealand) and bovine calf serum (BCS) (Abclone, Hurstbridge, Australia) was used. Polyvinylidene difluoride (PVDF) membrane was purchased from Millipore (Bedford, MA). The antibodies against C/EBPα, caspase-3, and β-actin were obtained from Santa Cruz Biotechnology (Dallas, TX). Antibodies against the PPARγ, AMPK α1+AMPK α2, anti-AMPK α1+AMPK α2, and cleaved caspase-3 were

purchased from Abcam (Cambridge, UK). The protein assay reagent (Bio-Rad, Vancouver, Canada) and the enhanced chemiluminescence (ECL) plus detection kit (Amersham, Buckinghamshire, UK) were used. All organic solvents used for HSCCC were of analytical grade and purchased from Duksan Pure Chemical Co. in Korea. Methanol of HPLC grade used for HPLC analysis and ESI-MS was supplied by J. T. Baker (Phillipsburg, NJ).

2.1.2. Sample preparation

Carduus crispus was collected from plants cultivated at the Medicinal Plant Garden, Natural Products Research Institute, Seoul National University and authenticated by Prof. Je Hyun Lee in Dongguk University. The dried *Carduus crispus* was cut with a grinder and extracted with methanol for 1 h by reflux. This procedure was repeated three times. The extracts were dried under reduced pressure using an N-1000s rotary evaporator (Eyela, Tokyo, Japan). The crude extract was divided into five liquid-liquid partition fractions according to polarity; hexane, ethyl acetate, chloroform, n-butanol, and water. These fractions were evaporated, freeze-dried and stored in a refrigerator prior to subsequent HSCCC separation (Figure 4).

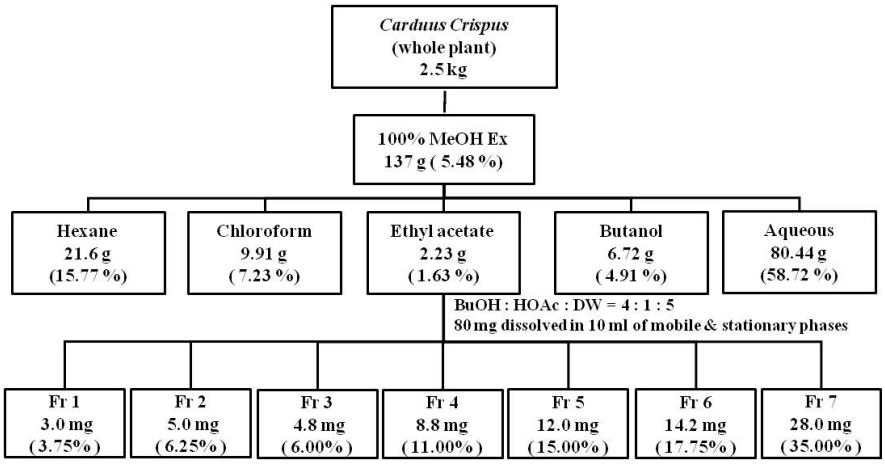

Figure 4. Schematic of the extraction and separation of the *Carduus crispus* extract.

The ethyl acetate layer is separated by EECCC using a solvent system of n-butanol-acetic acid-water (4:1:5, v/v). 80 mg of sample from CE was dissolved in 10 mL each of mobile and stationary phases. Ex.: extract, Fr: fraction, EECCC: Elution extrusion counter-current chromatography, CE: Ethyl acetate-soluble layer of the methanol extract from *Carduus crispus*

2.1.3. Apparatus

CO_2 incubator, clean bench and plate centrifuge (Vision Scientific, Korea), centrifuge (Hanil Scientific, Korea), multi-well plate reader (Molecular Devices, Emax, Sunnyvale, CA, USA), multi-well plate fluorometer (Molecular Devices, Gemini XS, Sunnyvale, CA, USA) were used. The HSCCC instrument was performed using a model TBE-300A high-speed counter-current-chromatography (Tauto Biotech, Shanghai, China) adopted three multilayered coil, 1.5 mm I.D. column (total volume 300 mL, sample loop 20 mL). The revolution speed of the apparatus can be regulated with a speed controller in the range between 0 and 1000 rpm. The system was also equipped with a model L-6200A constant-flow pump (Hitachi, Japan). Monitoring of the effluent was achieved with a SEDEX 55 ELSD (SEDERE, France). The peaks were collected with the model DC-1200 (Eyela, Japan). The HPLC equipment used was consisted of L-6200A pump (Hitachi, Japan), a SIL-9A auto injector (Shimadzu, Japan), a TC-50 controller, a SEDEX 75 ELSD (SEDERE, France) and a Spectra 100 UV detector (Spectra-Physics, Mount View, CA, USA). Most reaction products were purified by column chromatography. Diaion HP-20 resin (particle size 200-600 μm) was used for the column chromatography. ESI-MS experiments were conducted on an LCQ DECA XP ion-trap mass spectrometer (Thermo finnigan, San Jose, CA).

2.2. Methods

2.2.1. Cell culture

Mouse 3T3-L1 pre-adipocyte cells were obtained from the American Type Culture Collection (Manassas, VA). 3T3-L1 fibroblast cells were cultured in DMEM containing 10% BCS, 25 mM HEPES, 25 mM $NaHCO_3$, 100 units/mL of penicillin, and 100 μg/mL of streptomycin (growth medium) and incubated at 37 °C in 5% CO_2. After the cells were seeded at a density of 1.0 x 10^5 and reached confluence, they were grown for two days in growth medium. Cells were treated with the artificial hormonal inducer DMI (cocktail of 1 μM dexamethasone, 0.5 mM IBMX, and 1 μg/mL insulin) in DMEM containing 10% FBS (maintenance medium) for two days (from day 0 to day 2). After this treatment, the medium was changed to fresh maintenance medium with 1 μg/mL insulin and incubated for additional two days (from day 2 to day 4). Afterwards the medium was replaced with only maintenance medium every two day.

2.2.2. Cell viability assay

An MTT assay was used to measure cytotoxicity. Mouse 3T3-L1 fibroblast cells were detached from the cell culture flask by treatment with 0.05% trypsin and 0.53 mM EDTA. Cells were seeded at a density of 1.0 x 10^4 per well of a 96-well plate with 100 μL of growth medium and incubated

at 37 °C for 48 h until the cells reached confluence. They were replaced with new maintenance medium and incubated with various concentrations of samples for 48 h. After treatment, the medium was changed to 100 μL of MTT solution for 2 h. Violet formazan was dissolved in DMSO for 15 min. The plates were then measured at 595 nm with a microplate reader (Emax, Molecular Devices, Sunnyvale, CA).

2.2.3. Oil Red O staining

On day 8, the 3T3-L1 adipocytes were washed with D-PBS twice and fixed in filtered 10% formaldehyde in D-PBS for 1 h. Then, the cells were washed twice with distilled water, after which they were stained with filtered 0.5% Oil Red O solution (in 60% isopropanol) for 2 h at room temperature. Cells were washed with 60% isopropanol three times to remove unbound dye and observed with an inverted Leica fluorescence microscope at a magnification of 100x. Stained Oil Red O was eluted with elution solution (4% NP-40 in isopropanol, *v/v*) and quantified by measuring the optical absorbance at 490 nm.

2.2.4. Intracellular ROS

The level of intracellular ROS scavenging activity was assessed by using the oxidant-sensitive fluorescent probe, 2’ 7’- dichlorofluoresceine diacetate

(DCFA-DA) [50]. Dichloro-dihydro-fluorescein (DCFH) converted from dichloro-dihydro-fluorescein diacetate (DCFH-DA) by deacetylase within the cells is oxidized by a variety of intracellular ROS to dichloro-fluorescein (DCF), a fluorescent compound. 3T3-L1 adipocytes were seeded in a black 96-well plate. After 2 days, the cells were treated with indicated concentrations of pectolinarin with DMI. On day 8, the media was changed into *t*-BHP (200 μM) to induce ROS generation. After incubating the cells with DCFH-DA (20 μM) for 30 min, the fluorescence intensity was scanned by a 96-well microplate fluorometer (Molecular Devices Gemini XS, Sunnyvale, CA) and quantified by measuring the optical absorbance at 540 nm.

2.2.5. Western blot analysis

Mouse 3T3-L1 cells were washed once with ice-cold D-PBS, directly extracted with radioimmunoprecipitation assay (RIPA) buffer (20 mM Tris-Cl, pH 7.5, 150 mM NaCl, 1 mM Na_2EDTA, 1 mM EGTA, 1% NP-40, 1% sodium deoxy cholate, 2.5 mM sodium pyrophosphate, 1 mM Na_3VO_4, 1 mM dithiothreitol (DTT), 1 mM phenylmethanesulfonyl fluoride (PMSF), and a protein inhibitor cocktail; Sigma-Aldrich, St. Louis, MO) and incubated on ice for 30 min to promote lysis. After centrifuging at 14,000xg for 10 min, the protein content of the supernatant was measured, and aliquots (20 μg) of

protein were separated in SDS polyacrylamide gels and transferred to a PVDF membrane. After blocking with 5% skim milk, the membrane was incubated with primary and secondary antibodies, and the blot was developed for visualization using the ECL Plus detection kit. The intensity of each band was quantitatively determined using UN-SCAN-IT™ gel software (version 6.1, Silk Scientific, UT), and the density ratio showed the relative intensity of each band compared with the controls in each experiment.

2.2.6. Statistical analysis

Values were expressed as the mean ± standard deviation (S.D.). The statistical significance of the differences between the study groups was assessed by analysis of variance (ANOVA) followed by Student's t-test (SPSS version 10.0, Chicago, IL). The proportion of Oil Red O positive cells per well was measured in triplicate for each treatment on three separate occasions. Significance was assessed as $p < 0.05$ [$*p < 0.05$; $**p < 0.01$; $***p < 0.005$].

3. Results

3.1. Inhibitory effect of the *Carduus crispus* methanol extract on lipid accumulation in 3T3-L1 Cells

The effect of *Carduus crispus* extract on a product of lipid accumulation indicative of 3T3-L1 differentiation was examined by Oil Red O staining. To evaluate the anti-obesity effects of the *Carduus crispus* extract, a comparison with the known PPARγ antagonist GW9662 was performed. Figure 5A shows the results of Oil Red O staining under a microscope. Quantitatively, treatment of 3T3-L1 adipocytes with *Carduus crispus* at 100 μg/mL showed a significant decrease in lipid accumulation in differentiated adipocytes by 40.0±1.0% ($p < 0.005$). To investigate the key regulators of adipogenesis, PPARγ and C/EBPα protein expression levels in 3T3-L1 cells were measured by Western blot analysis. Figure 5B shows that the *Carduus crispus* methanol extract inhibited over 60% of PPARγ protein expression at a concentration of 50 μg/mL and inhibited over 50% of C/EBPα expression at a concentration of 25 μg/mL in maturing pre-adipocytes.

A

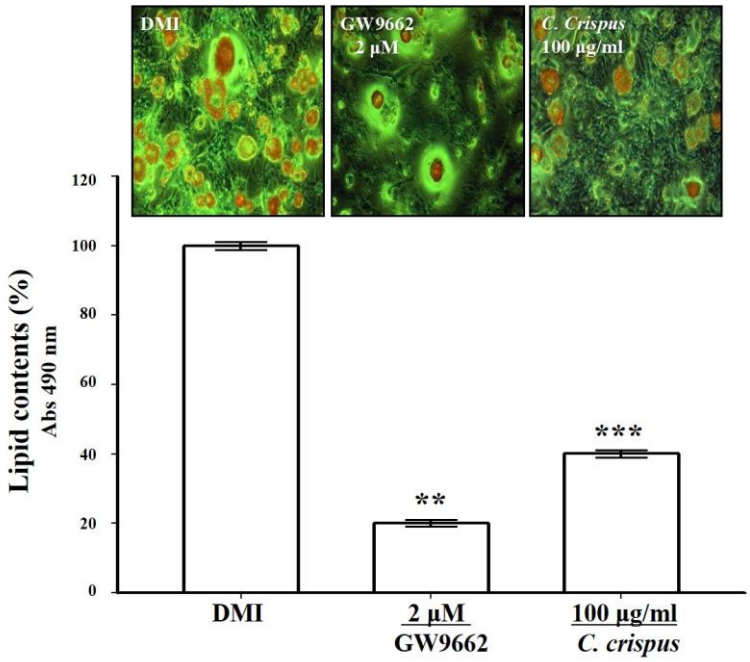
DMI
GW9662
2 μM
C. Crispus
100 μg/ml
Lipid contents (%)
Abs 490 nm
120
100
80
60
40
20
0
**
***
DMI
2 μM
GW9662
100 μg/ml
C. crispus

B

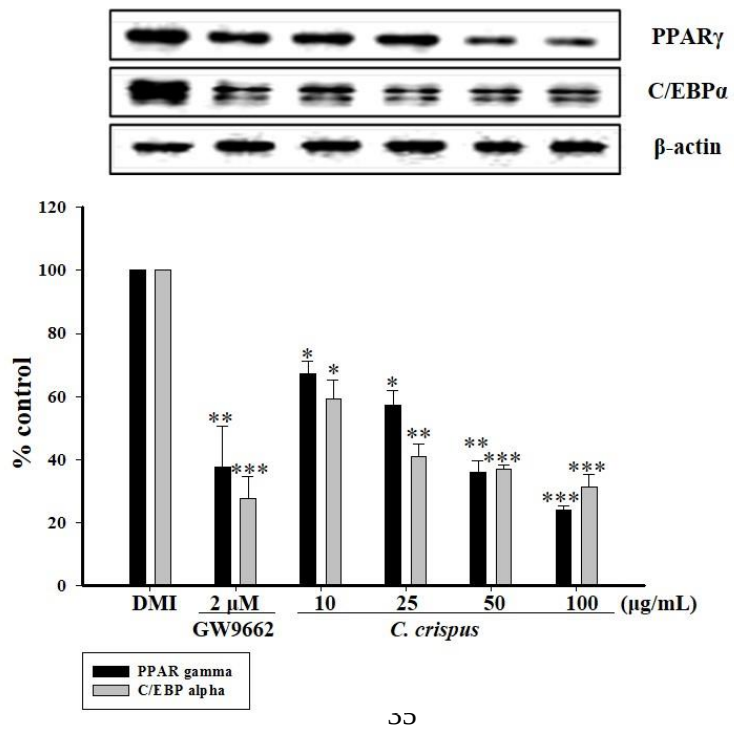
PPARγ
C/EBPα
β-actin
% control
120
100
80
60
40
20
0
DMI
2 μM
GW9662
10
25
50
100
(μg/mL)
C. crispus
PPAR gamma
C/EBP alpha

Figure 5. Inhibitory effects of the *Carduus crispus* methanol extract on lipid accumulation and PPARγ and C/EBPα protein expression during adipogenesis.

Mouse 3T3-L1 pre-adipocyte cells were differentiated with DMI in either the absence or presence of 100 μg/mL of *Carduus crispus* extract on lipid accumulation and various concentrations of *Carduus crispus* extract on the protein expression of principal adipogenic factors. (A) After this treatment for eight days, the cells were stained with Oil Red O followed by elution of the stained Oil Red O with 4% NP-40 solution, and the stained lipid content was quantified by measuring absorbance at 490 nm; (B) To examine the expression levels of PPARγ and C/EBPα, the cells were lysed on day 5. β-actin was used as an internal reference for sample loading control. Densitometric quantitation for PPARγ and C/EBPα was performed. All of the experiments were performed in triplicate, and the results are represented as the mean ± S.D. DMI: Cocktail of 1 μM dexamethasone, 0.5 mM IBMX and 1 μg/mL insulin

3.2. Effects of the five liquid layers from *Carduus crispus* methanol extract on the expression of PPARγ and C/EBPα proteins in 3T3-L1 cells

After solvent fractionation of *Carduus crispus*, the CH (hexane-soluble layer), CC (chloroform-soluble layer), CE (ethyl acetate-soluble layer), CB (*n*-butanol-soluble layer), and CW (water-soluble layer) were obtained from the methanol. We compared the inhibitory effects of every fraction from *C. crispus* on the production of PPARγ and C/EBPα. All of the fractions except for the CB drastically decreased PPARγ expression. As shown in Figure 6, DMI-induced PPARγ and C/EBPα protein expressions are strongly inhibited by the CE layer (18.0% and 39% of DMI, respectively). The CB fraction had no effect on the C/EBPα protein expression, but there was a 50% decrease in the protein expression of C/EBPα in the CC and CE layers.

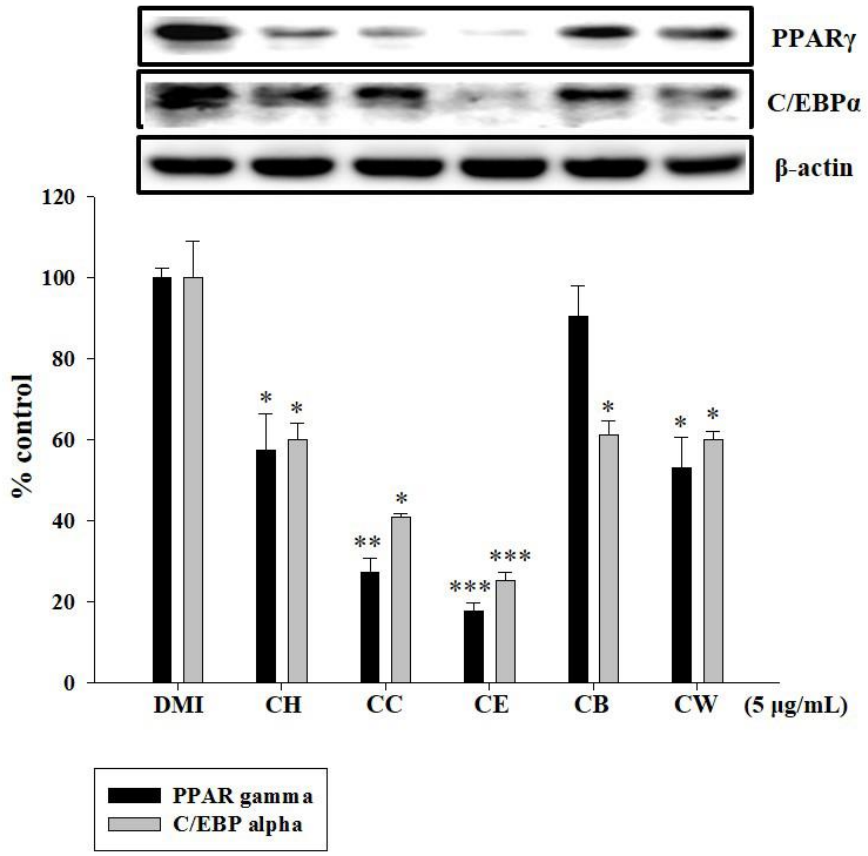

Figure 6. Inhibitory effects of different fractions from *Carduus crispus* on PPARγ and C/EBPα protein expression during adipogenesis.

Mouse 3T3-L1 pre-adipocyte cells were differentiated with DMI in either the absence or presence of 5 μg/mL of each fraction. To examine the expression levels of PPARγ and C/EBPα, the cells were lysed on day 5. β-actin was used as an internal reference for sample loading control. Densitometric quantitation for PPARγ and C/EBPα was performed. All of the experiments were performed in triplicate, and the results are represented as the mean ± S.D. DMI: Cocktail of 1 μM dexamethasone, 0.5 mM IBMX and 1 μg/mL insulin,

CH: Hexane-soluble layer of the methanol extract from *C. crispus*, CC: Chloroform-soluble layer of the methanol extract from *C. crispus*, CE: Ethyl acetate-soluble layer of the methanol extract from *C. crispus*, CB: *n*-Butanol-soluble layer of the methanol extract from *C. crispus*, CW: Water-soluble layer of the methanol extract from *C. crispus*

3.3. Selection of the two-phase solvent system on EECCC

Under the optimum conditions, seven fractions were obtained in the one-step EECCC, as shown in Figure 7. The *K* values about several peaks are given in Table 1. Among these fractions, two components were identified: 12 mg of fraction 5 (collected during 495–530 min) and 14.2 mg of fraction 6 (collected during 620–640 min). The purities of these components were 94.6% and 91.9%, respectively, as determined by the HPLC peak area percentage. Among these fractions, two components were identified: 12 mg of fraction 5 (collected during 495–530 min, 15.00% yield) and 14.2 mg of fraction 6 (collected during 620–640 min, 17.75% yield). The purities of these components were 94.6% and 91.9%, respectively, as determined by the HPLC peak area percentage. The *K* values about several peaks are given in Table 1.

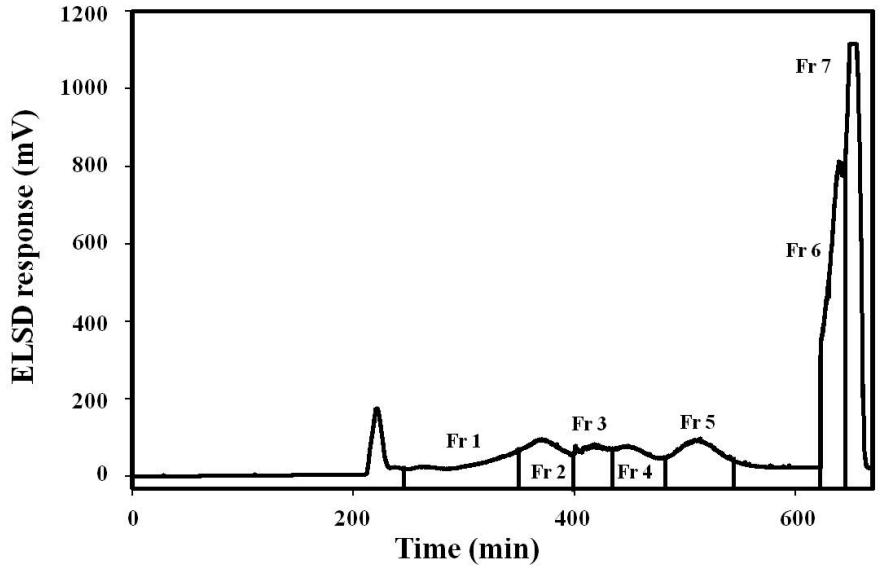

Figure 7. The HSCCC chromatograms of the EA extract from *Carduus crispus*.

Solvent system: *n*-butanol/acetic acid/water (4:1:5 v/v/v); stationary phase: upper phase; mobile phase: lower phase; flow rate: 1 mL/min for 390 min, 2 mL/min for 390-600 min and 1 mL/min for the remaining time; sample size: 80 mg. ELSD detection: nebulizer gas flow rate: 2.5 L/min, drift tube temperature: 90°C, split ratio: 10:1. Fr: fraction. HSCCC: High speed counter-current chromatography

Table 1. Partition coefficient (*K*) values of *Carduus crispus* in different solvent systems.

Solvent composition	Peak1	Peak2	Peak3	Peak 5	Peak4	Peak 6	Peak7
EaMAcW (5:1:0.5:5)	2.71			4.03	5.07	32.66	
EaMW (5:1.5:5)	2.56			4.06	6.40	55.09	56.28
EaMHoacW (4:1:0.25:5)	2.80			5.93	9.74	144.45	
BEaW (4:1:5)	78.8			73.9			
BEaW (3:2:5)			4.14	88.55	91.85		
EaMW (3:2:5)	2.18	1.25	1.19	4.49	7.15	177.36	
EaMW (4:1:5)	3.28		1.48	31.42	22.03		
EaMW (5:1:5)	3.86		2.07	10.99	44.80		
BHoacW (4:1:5)	3.42	5.82	2.01	4.57	6.65	18.13	
BHoacW (4:0.5:5.5)	14.37	38.62	42.99	18.91			
BW (4:6)	79.56		41.78	87.96			

BW (5:5)	-					
BHoacW (4.5:0.5:5)	26.96					
BHoacW (4.5:1:4.5)	10.25	31.74	18.29	13.45	25.21	127.85

The *K* value is calculated by peak area of each solute at the lower phase divided into that at the upper phase. Ac: acetone, B: n-butanol, Ea: ethyl acetate, Hoac: acetic acid, M: methanol, W: distilled water

3.4. Structural identification

The structural identification of two fractions was performed by use of ESI-MS (negative ion mode) and 1H-NMR spectroscopy. Data of each compound were as follows: Fraction 5 in Figure 7: ESI-MS(m/z): 431.1([M-H]$^-$), 284.1([M-H-rha]$^-$), 456.8([M-H-2H2O]$^-$), 862.7(2[M-H]$^-$), 1294.2(3[M-H]$^-$). 1H NMR(500 MHz, CD3OD) 0.9 (d, J = 6 Hz, CH3), 5.33 (1H, d, J = 1.5 Hz, H-1'), 6.2 (1H, d, J = 2.5 Hz, H-6), 6.77 (1H, d, J = 2.5 Hz, H-8), 6.93 (2H, d, J = 8.4 Hz, H-3' and H-5'), 7.76 (2H, d, J = 8.4 Hz, H-2' and H-6'). The results were matched to literature data for kaempferol-rhamnoside [51]. Fraction 6 in Figure 7: ESI-MS(m/z): 269.3([M-H]$^-$), 538.6(2[M-H]$^-$). By comparing the retention time and the molecular weight identified by ESI-MS, fraction 6 was confirmed as apigenin.

3.5. Effects of the EECCC fractions from the EA-soluble layer of *Carduus crispus* on lipid accumulation in 3T3-L1 cells

Because the CE layer reduced the expression of PPARγ and C/EBPα proteins in 3T3-L1 adipocytes, we attempted to identify the main component responsible for this activity. All of the fractions (5 μg/mL) obtained by EECCC showed no cytotoxicity in the MTT assay (data not shown). A total of seven fractions from the CE layer were compared by Oil Red O staining, and both fraction 2 and fraction 6 showed the positive activity, as shown in Table 2. The inhibitory effect of fraction 6 (59% inhibition) was 6% higher than the effect of fraction 2 (53%). Although fraction 2 showed a significant effect, we confirmed with ESI-MS and assured that it is not a single compound. Therefore it has been focused on fraction 6 which demonstrated the highest activity.

Table 2. Inhibitory effects of each fraction from EECCC on lipid accumulation in 3T3-L1 adipocytes.

	Lipid contents (%)
DMI	100.0 ± 12.63
Fraction 1	62.9 ± 7.64
Fraction 2	46.1 ± 1.38*
Fraction 3	119.1 ± 8.81
Fraction 4	97.0 ± 8.63
Fraction 5	70.6 ± 1.49
Fraction 6	40.9 ± 3.32*
Fraction 7	72.9 ± 1.31

All of the samples were used at a concentration of 5 μg/mL. Data are represented as the mean ± S.D ($p < 0.05$). Significance was assessed as $p < 0.05$ [*$p < 0.05$; **$p < 0.01$; ***$p < 0.005$].

3.6. Effects of apigenin on the cell viability and accumulation of lipid droplets in 3T3-L1 cells

The effects of apigenin on cell viability and adipogenesis using 3T3-L1 cells. In maturing preadipocytes, after 5 days treatment, 10 and 50 μM apigenin decreased cell viability dose-dependently by 102.2 ± 1.4%, and 72.4 ± 0.5% ($p < 0.005$), respectively and in mature adipocytes, after 8 days treatment, 10 and 50 μM apigenin decreased cell viability dose-dependently by 80.7 ± 3.6%, and 45.7 ± 0.7% ($p < 0.005$), respectively (Figure 8A). The inhibitory effect of apigenin on the expression of adipogenic markers resulted in a diminished accumulation of lipids in the cells, which was confirmed by the Oil Red O staining. As shown in Figure 8B, treating the cells with DMI induced an increase in lipid droplet production, which was inhibited by treatment with 40 μM of apigenin (76.9% inhibition). This inhibition was more pronounced compared with treatment with the PPARγ antagonist, GW9662.

3.7. Effects of apigenin from the EA layer of *Carduus crispus* on the expression of proteins associated with differentiation induction

The effect of apigenin on protein levels of PPARγ and C/EBPα associated with differentiation induction in adipocytes compared with

GW9662 (Figure 8C). In undifferentiated cells (control), PPARγ and C/EBPα protein expression was not detected. After treatment with DMI, PPARγ and C/EBPα expression levels were greatly increased. However, treatment with 40 μM of apigenin reduced the protein expression levels of PPARγ and C/EBPα by 66.5% and 77.9%, respectively. Our results showed that apigenin attenuated lipid accumulation and the phosphorylation of AMPK increased in a dose-dependent manner on differentiated 3T3-L1 cells (Figure 8D). Caspase-3 activity was also evaluated by Western blot analysis, as it is the primary indicator of apoptotic cell death. Apigenin was shown to induce apoptosis with an increase of cleaved caspase-3 specifically in maturing 3T3-L1 adipocytes.

A

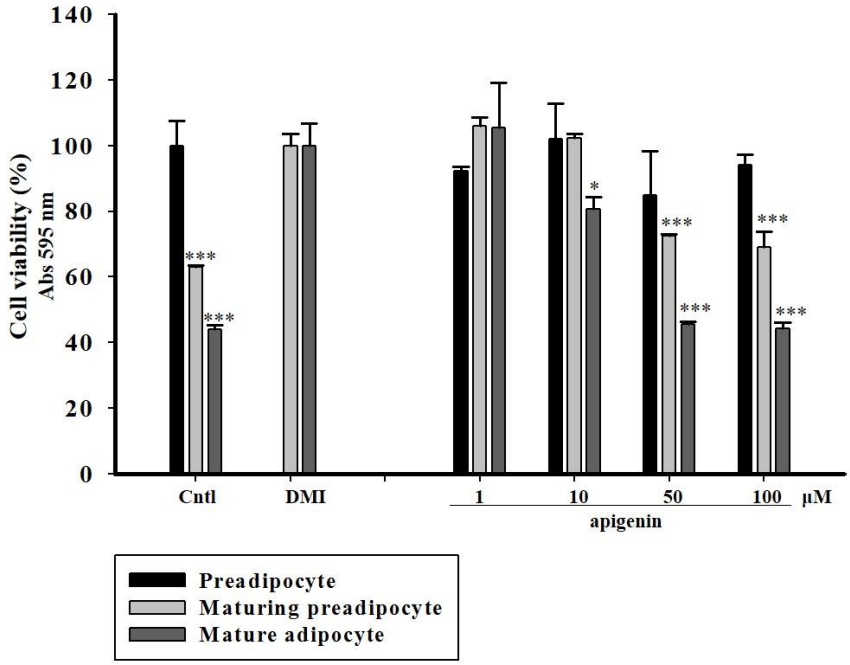
Cell viability (%)
Abs 595 nm
140
120
100
80
60
40
20
0
***
***
*
***
***
***
***
Cntl
DMI
1
10
50
100
μM
apigenin
Preadipocyte
Maturing preadipocyte
Mature adipocyte

B

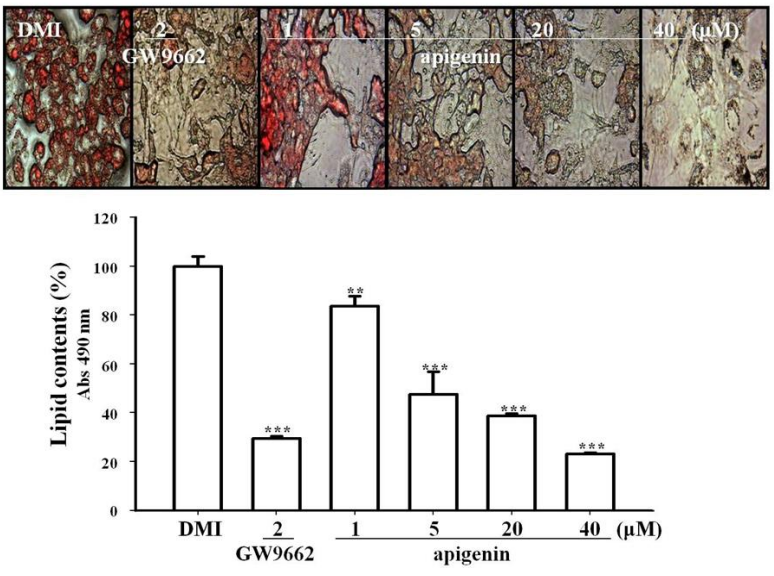
DMI
2
GW9662
1
5
apigenin
20
40 (μM)
Lipid contents (%)
Abs 490 nm
120
100
80
60
40
20
0
**
***
***
***
***
DMI
2
GW9662
1
5
20
40 (μM)
apigenin

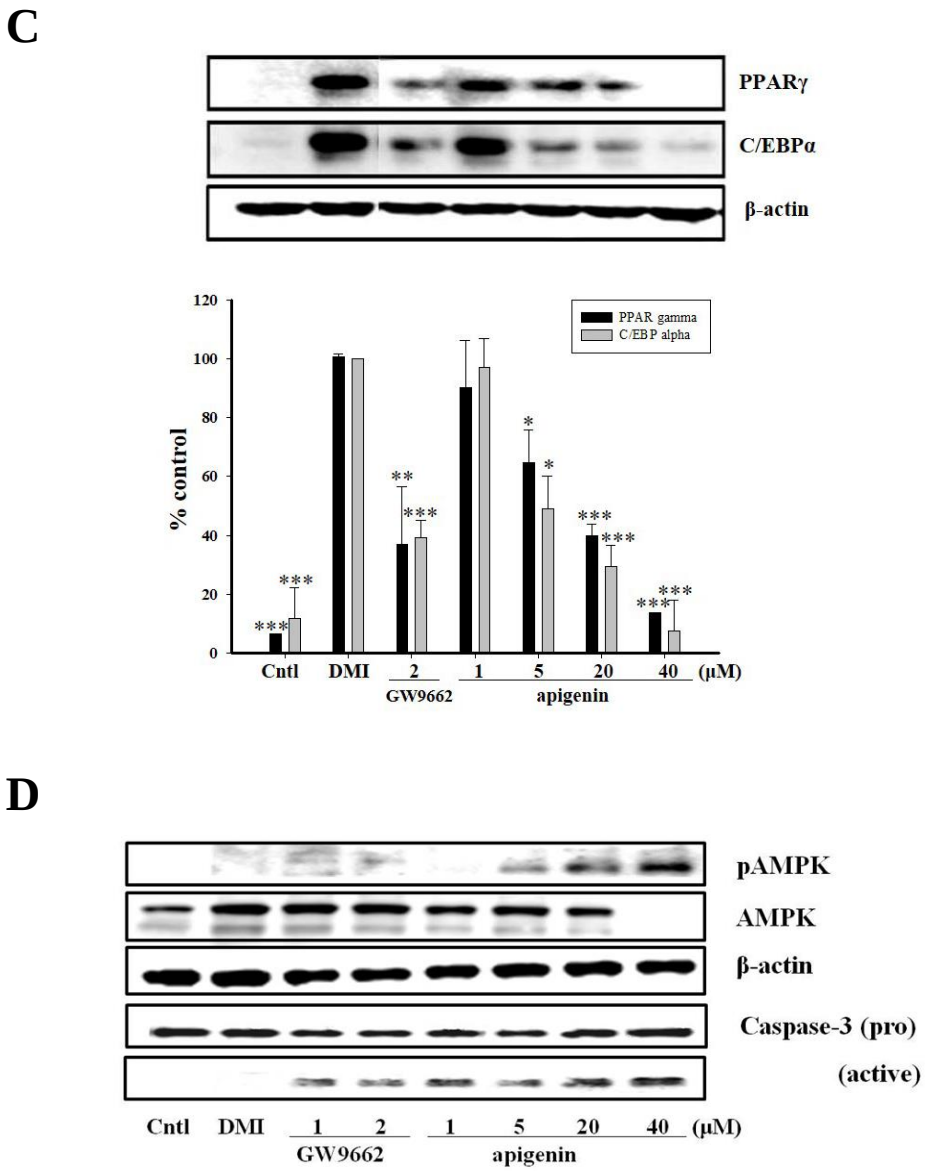

Figure 8. Inhibitory effects of apigenin extracted from *Carduus crispus* on lipid accumulation and induction of differentiation and apoptosis in 3T3-L1 mature adipocytes.

Mouse 3T3-L1 pre-adipocyte cells were differentiated with DMI in either the absence or presence of 1, 5, 20, and 40 μM of apigenin. (A) After five days

and eight days at the same conditions with maturing preadipocytes and mature adipocytes, an MTT assay was used to measure cell viability. After 100 μL of MTT solution treatment, violet formazan was dissolved in DMSO and measured at 595 nm; (B) After this treatment for eight days, the cells were stained with Oil Red O followed by elution of the stained Oil Red O with 4% NP-40 solution, and the stained lipid content was quantified by measuring absorbance at 490 nm; (C) On day 5, the cells were lysed to examine the expression levels of PPARγ and C/EBPα. Cleaved caspase-3 was also detected in the same protein lysate. Densitometric quantitation for PPARγ and C/EBPα was performed; (D) After treatment with DMI for eight days, the expression of the phosphorylated and pro-forms of AMPK and caspase-3 were detected. β-actin was used as an internal control. All of the experiments were performed in triplicate, and the results are represented as the mean ± S.D. DMI: Cocktail of 1 μM dexamethasone, 0.5 mM IBMX and 1 μg/mL insulin

3.8. Effects of pectolinarin from *Cirsium japonicum* on lipid accumulation in 3T3-L1 cells

The inhibitory effect of pectolinarin on the expression of adipogenic markers resulted in a diminished accumulation of lipid droplets in 3T3-L1 mature adipocytes, which was confirmed by the Oil Red O staining. As shown in Figure 9A, treating the cells with DMI induced an increase in lipid droplet production, which was inhibited by treatment with pectolinarin in a dose-dependent manner. This inhibition was more pronounced compared with treatment with the PPARγ antagonist, GW9662. Pectolinarin did not induce cell death in the 3T3-L1 pre-adipocyte and mature adipocytes.

3.9. Effects of pectolinarin from *Cirsium japonicum* on intracellular ROS generation in 3T3-L1 cells

The inhibitory effect of pectolinarin on t-BHP-induced ROS in 3T3-L1 adipocyte was evaluated (Figure 9B). Pectolinarin showed a significant reduction of ROS production in a dose-dependent manner.

3.10. Effects of pectolinarin from *Cirsium japonicum* on the Expression of Proteins Associated with Differentiation Induction

The effects of pectolinarin on protein levels of PPARγ and C/EBPα

associated with differentiation induction in adipocytes were compared with GW9662 (Figure 9C). After treatment with DMI and pectolinarin, treatment with pectolinarin reduced the protein expression levels of PPARγ and C/EBPα against DMI only.

Figure 9D showed that the phosphorylation of AMPK increased in a dose-dependent manner on differentiated 3T3-L1 cells. Caspase-3 activity was also evaluated by Western blot analysis. However, pectolinarin was not shown the increase of cleaved caspase-3 in maturing 3T3-L1 adipocytes (data not shown). To understand the molecular events of decreased lipid accumulation in cells exposed to the pectolinarin, SREBP-1 protein levels were also evaluated. SREBP-1 protein level was greatly reduced at pectolinarin concentration of 50 μM. Next, the result of heme oxygenase (HO)-1 protein expression, associated with intracellular ROS generation by the oxidative stress, was detected that pectolinarin reduced expression level of the HO-1.

A

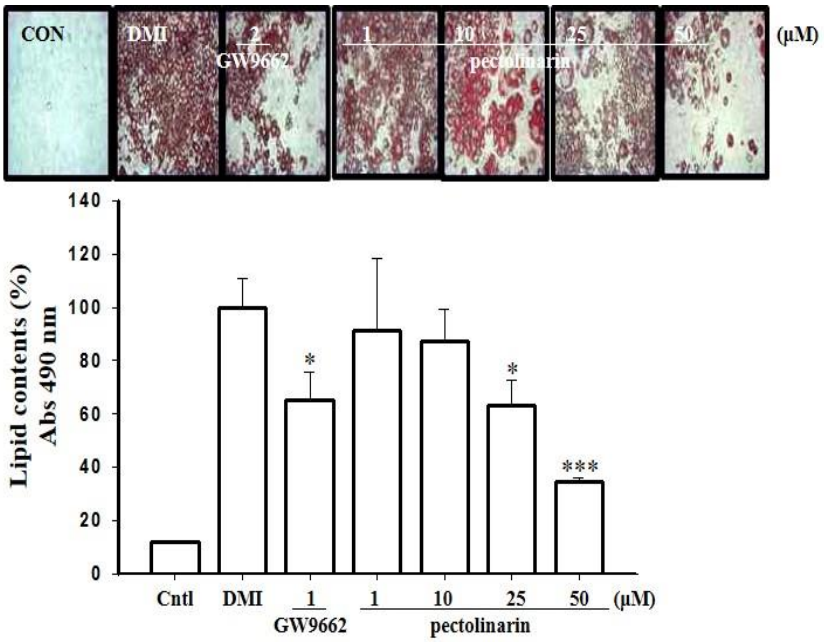
CON
DMI
2
GW9662
1
10
25
50
(μM)
pectolinarin
Lipid contents (%)
Abs 490 nm
140
120
100
80
60
40
20
0
*
*
***
Cntl
DMI
1
1
10
25
50
(μM)
GW9662
pectolinarin

B

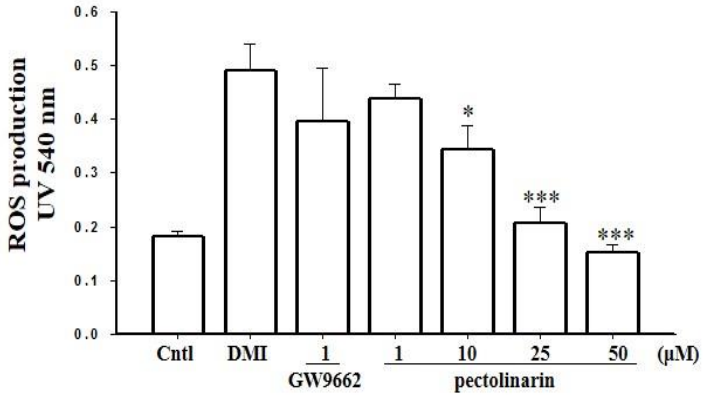
ROS production
UV 540 nm
0.6
0.5
0.4
0.3
0.2
0.1
0.0
*
***
***
Cntl
DMI
1
1
10
25
50
(μM)
GW9662
pectolinarin

C

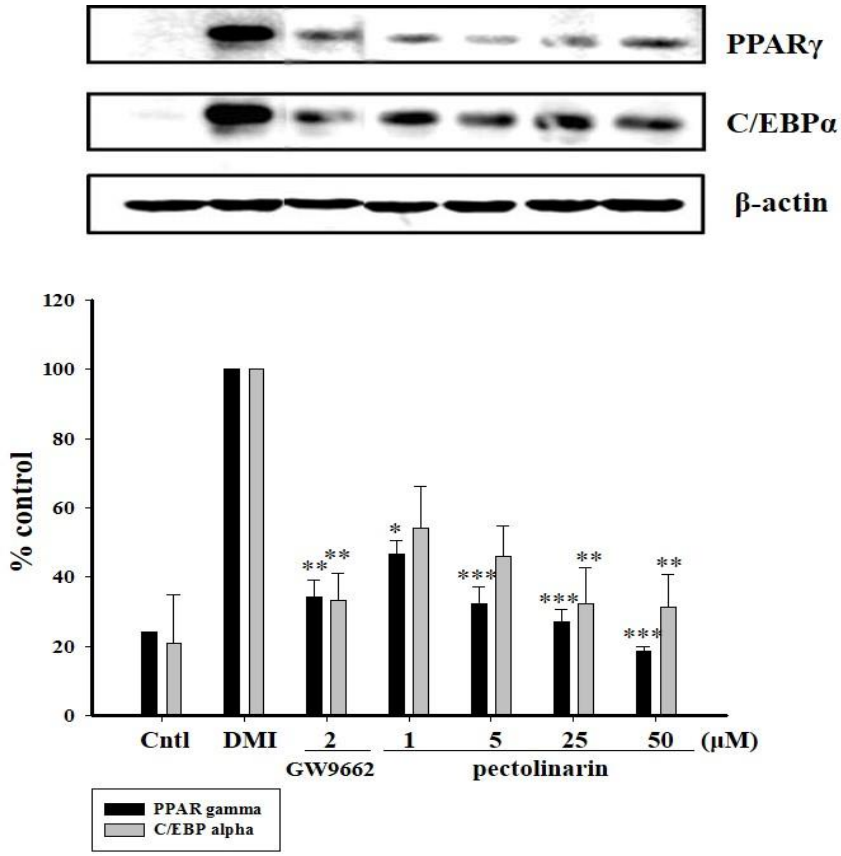
PPARγ
C/EBPα
β-actin
120
100
80
60
40
20
0
% control
**
**
*
***
***
**
***
**
Cntl
DMI
2
1
5
25
50
(μM)
GW9662
pectolinarin
PPAR gamma
C/EBP alpha

D

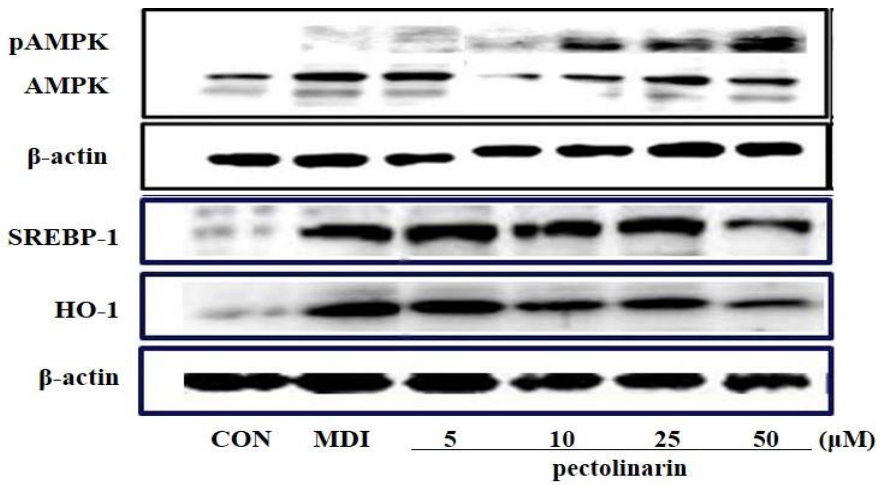
pAMPK
AMPK
β-actin
SREBP-1
HO-1
β-actin
CON
MDI
5
10
25
50
(μM)
pectolinarin

Figure 9. Inhibitory effects of pectolinarin extracted from *Cirsium japonicum* on lipid accumulation and induction of lipid oxidation in 3T3-L1 adipocyte cells.

Mouse 3T3-L1 pre-adipocyte cells were differentiated with DMI in either the absence or presence of 1, 10, 25, and 50 μM of pectolinarin. (A) After this treatment for eight days, the cells were stained with Oil Red O followed by elution of the stained Oil Red O with 4% NP-40 solution, and the stained lipid content was quantified by measuring absorbance at 490 nm.; (B) On day 8, the cells were lysed to examine the intracellular ROS generation.; (C) On day 5, the cells were lysed to examine the expression levels of PPARγ and C/EBPα.; (D) SREBP-1 and HO-1 were also detected in the same protein lysate. After treatment with DMI for eight days, the expression of the phosphorylated and pro-forms of AMPK were detected. β-actin was used as an internal control. All of the experiments were performed in triplicate, and the results are represented as the means ± S.D. Significance was assessed as $p < 0.05$ [*$p < 0.05$; **$p < 0.01$; ***$p < 0.005$].

4. Discussion

Adipogenesis is promoted by increased expression of the PPARγ and C/EBPα genes [52]. PPARγ acts as a transcription factor to several genes associated with differentiation [53]. Although the gene levels and protein levels of PPARγ and C/EBPα are very low in 3T3-L1 pre-adipocytes, increased expression levels accompany the differentiation caused by various inducers [54, 55]. By day 5, *Carduus crispus* had suppressed the expression of the adipocyte differentiation makers PPAR-γ and C/EBPα.

The purpose of this study was to isolate and identify the active compound(s) from the methanol extract of the *Carduus crispus* plant that has shown an inhibitory effect on adipogenesis in 3T3-L1 cells. Studying the cytotoxicity of *Carduus crispus* against 3T3-L1 cells by the MTT assay showed no toxicity at concentrations up to 100 μg/mL; therefore, the maximum concentration of *Carduus crispus* used in the present study was 100 μg/mL. This result implies that *Carduus crispus* is not associated with blocking clonal expansion in the early stage of pre-adipocytes. Under the bioassay-guidance of anti-obesity activity according to lipid accumulation and Western blot analysis for PPARγ and C/EBPα in differentiated 3T3-L1 cells, the sub fractions from the extract and subsequent compounds with the highest activity were selected. The results showed that the CE of the *Carduus crispus* extract, the flavonoid-rich fraction, resulted in the strongest inhibition of

adipogenesis activity on 3T3-L1 cells by decreasing protein expression of adipogenic transcription factors PPARγ and C/EBPα without cytotoxicity at a concentration of 5 μg/mL. Therefore, we isolated the compounds of the CE layer using EECCC and HPLC-UVD systems to confirm the active component. After comparing the different ratios of the *K* value, *n*-butanol-acetic acid-water (4:1:5, v/v) resulted in the best separation. However, the *K* value of peak 6 (fraction 6) was too high to separate the compounds. Therefore, EECCC was used to reduce the amount of time necessary to separate the analyte. From these efforts, five mixtures and two isolated compounds were obtained. Fraction 5 and 6 were identified as kaempferol-rhamnoside and apigenin, respectively, which were confirmed by ESI-MS and 1D-NMR.

Finally, apigenin (fraction 6) is the main bioactive compound from *Carduus crispus* on adipogenesis. Apigenin exhibited a promising anti-adipogenic effect against lipid accumulation, PPARγ and C/EBPα protein expression, and for the activation of AMPK protein expression. AMPK activation, a metabolic master switch, induced apoptotic cell death, inhibition of lipolysis, and the down-regulation of key adipogenic genes such as PPARγ and C/EBPα [56].

Apigenin is found not only in species of genus *Carduus* but also in a number of other vegetables and fruits, such as parsley, onions, chamomile,

orange, and some seasonings. Apigenin also possesses anti-inflammatory, anti-carcinogenic, and free radical scavenging properties [57, 58]. It has been reported that apigenin is a potent inhibitor of the activation of nuclear transcription factor NF-κB, which has been associated with the regulation of cell growth, cell-cycle regulation, and apoptosis [59]. Studies in several human carcinoma cell lines, including breast cancer, colon cancer, and leukemia, have shown that apigenin induces growth inhibition, cell cycle arrest, and apoptosis [60, 61]. In this study, apigenin resulted in the induction of apoptosis not only in several cancer cells but also in 3T3-L1 cells as evidenced by cleaved caspase-3 detection. Apoptosis in mature adipocytes was attributed to the diminished accumulation of lipids.

In summary, the methanol extract of *Carduus crispus* has an inhibitory effect on adipogenesis in 3T3-L1 adipocyte cells. The CE contained abundant flavonoids and attenuated the main regulatory factors of adipogenesis, PPARγ and C/EBPα. We obtained two pure compounds from this fraction though EECCC: kaempferol-rhamnoside and apigenin. Because of the potent inhibition of adipogenesis by apigenin, we anticipate that *Carduus crispus* and its constituent, apigenin, will be useful for the treatment of undesired weight gain and metabolic diseases, including disorders related to lipid metabolism. This is the first report showing that apigenin, as one of the main bioactive compounds in *Carduus crispus*, exerts apoptotic activity on 3T3-L1 cells. For

this reason, it could be asserted that *Carduus crispus* has potent anti-adipogenic activity.

Using the marker substance pectolinarin, isolated from *Cirsium japonicum*, another representative type of plant belonging to the group of thistles, a dose-dependent decrease on lipid accumulation was identified in 3T3-L1 adipocytes. This inhibitory effect on adipogenesis was shown to be induced by the suppression of a sterol regulatory element SREBP-1 and the activation of AMPK. The findings that the generation of ROS and the expression of HO-1 proteins were inhibited suggest that this anti-adipogenic effect resulted from lipid oxidation.

The present study demonstrates that apigenin from *Carduus crispus* and pectolinarin from *Cirsium japonicum* have reduced the lipid accumulation with their significantly inhibition of PPARγ and C/EBPα protein expressions and the activation of AMPK. However, apigenin has cytotoxicity at 50 μM not in pre-adipocytes but in mature adipocytes and pectolinarin has no cytotoxic effect on both types of cells. In summary, this study shows that apigenin has shown the apoptotic 3T3-L1 cell death via the activation of AMPK and caspase-3. Whereas pectolinarin, against apigenin, has shown the lipid oxidation via the inhibition of intracellular ROS and HO-1 generation.

CHAPTER II.

Optimization of headspace-solid phase micro extraction coupled to gas chromatography mass spectrometer for the chemical composition analysis of chamomile (*Matricaria recutita* L.) and bioactivity-guided isolation of its anti-inflammatory active components

1. Introduction

1.1. Inflammation

The cause of inflammation is unknown, although there are several theories. Most of them assert that RA is traditionally considered a chronic, inflammatory autoimmune disorder that causes the immune system to attack the joints. It is a disabling and painful inflammatory condition, which can lead to substantial loss of mobility due to pain and joint destruction. Within the past few years, greater understanding of the pathophysiology of RA has permitted development of therapies targeted at specific cytokines. Tumor necrosis factor-alpha (TNF-α), interleukin-1β (IL-1β), interleukin-6β (IL-6β), and interleukin-8β (IL-8β) are pro-inflammatory cytokines believed to play a key role in the inflammatory response in RA [62]. In response to these cytokines, NF-κB transcription factor controls the expression of a plethora of genes involved in inflammation, anti-apoptosis, and cell proliferation [63].

RA usually requires lifelong treatment, including medications, physical therapy, exercise, education, and possibly surgery. Early, aggressive treatment for RA can delay joint destruction. Anti-inflammatory agents used to treat RA include aspirin and non-steroidal anti-inflammatory drugs (NSAIDS), such as ibuprofen (Motrin, Advil), fenoprofen, indomethacin, and naproxen (Naprosyn). NSAIDS are commonly used to relieve joint pain and inflammation. Although NSAIDs work well, long-term use can cause stomach

problems, such as ulcers and bleeding, and possible heart problems. COX-2 inhibitors block an inflammation-promoting enzyme called COX-2. This class of drugs was initially believed to work as well as traditional NSAIDs, but with fewer stomach problems. However, numerous reports of heart attacks and stroke have prompted to re-evaluate the risks and benefits of the COX-2s. Rofecoxib (Vioxx) and valdecoxib (Bextra) have been withdrawn following reports of heart attacks in patients taking the drugs. Celecoxib (Celebrex) is still available, but labeled with strong warnings and a recommendation that it be prescribed at the lowest possible dose for the shortest duration possible. Other drugs that suppress the immune system, such as azathioprine (Imuran) and cyclophosphamide (Cytoxan), are sometimes used in people who have failed other therapies. These medications are associated with toxic side effects and usually reserved for severe cases of RA. Because of these problems, a major target of drug research is the development of NSAIDs with anti-inflammatory and analgesic activity but without side effects.

1.2. *Matricaria recutita* L.

1.2.1. German chamomile

chamomile has been used for centuries as a medicinal plant mostly for its anti-inflammatory, analgesic, anti-microbial, anti-spasmic and sedative properties [64, 65]. As a member of Asteraceae family, it is widely

represented by two known varieties viz. German chamomile (*Matricaria chamomilla*) and Roman chamomile (*Chamaemelum nobile*). German chamomile in particular is the most common variety used for medicinal purpose [65]. It is known to contain several classes of biologically active compounds including essential oils and several polyphenols. The principal components of the essential oil extracted from chamomile flowers are the terpenoids α-bisabolol and its oxide, azulenes including chamazulene and acetylene derivatives [66]. Terpenoids, bisabolol, and chamazulene have been shown to possess anti-inflammatory, anti-allergic, antispasmodic, antibacterial, antipyretic, ulcer-protective, and antifungal properties [65]. Numerous reports are available on the identification of several phenolic compounds including apigenin, quercetin, and patuletin as glucosides and various acetylated derivatives [67, 68]. In natural conditions most of the flavonoids occur as glucosides bound to the sugar moiety. Glucosides are highly stable and water soluble. In fact, infusion is one of the most popular methods and has been traditionally used as carminative and mild sedative to calm nerves and reduce anxiety, to treat hysteria, nightmares, insomnia, and other sleep problems. Additionally, chamomile has been valued as a digestive relaxant and has been used to treat various gastrointestinal disturbances including flatulence, indigestion, diarrhea, anorexia, motion sickness, nausea, and vomiting [69, 70]. The widespread use and medicinal properties has made chamomile

increasingly popular in the form of tea which is consumed at a rate of over one million cups per day. Apart from the existing traditional knowledge on tis therapeutic efficacy more work has been conducted in recent years on chamomile to establish its antioxidant, hypocholesterolemic, anti-parasitic, and anti-aging properties [71-74].

The present study is evaluated anti-inflammatory properties of chamomile of methanol extract to identify its essential oil and anti-inflammatory compound.

1.2.2. Essential oils

Essential oils are valuable natural products used as raw materials in many fields, including perfumes, cosmetics, aromatherapy, phytotherapy, spices and nutrition [75]. Aromatherapy is the therapeutic use of fragrances or at least mere volatiles to cure, mitigate or prevent diseases, infections and indispositions by means of inhalation [76]. This has recently attracted the attention of many scientists and encouraged them to screen plants to study the biological activities of their oils from chemical and pharmacological investigations to therapeutic aspects. Hopefully, this will lead to new information on plat applications and new perspective on the potential use of these natural products.

1.3. HS-SPME/GC-MS

Because the emitted volatile fraction plays a fundamental role in a plant's life, various novel techniques have been developed for its extraction from plants. In essential oil analysis, gas chromatography (GC) techniques are used as the main analytical method because the majority of essential oils are volatiles. Volatile compounds are usually isolated from sample matrix by using several sample preparation techniques, *e.g.* liquid phase extraction, gas phase extraction/distillation and solid phase extraction, before GC analysis. Sample pretreatment procedure is very important for GC-MS technique. Most of the time, it deals with the organic solvent, which may cause environmental pollution and be hazardous to health. Therefore, developing environmentally benign pretreatment procedures are highly desirable. The essential oils of aromatic herbs are traditionally obtained using steam distillation [77-79] and organic solvent extraction using percolation, maceration or Soxhlet techniques [80-82]. These procedures, however, have distinct drawbacks such as time-consuming and labor-intensive operations, handling of large volumes of hazardous solvents and extended concentration steps with can result in the loss or degradation of target analytes [83]. One novel technique that should be suitable for volatile arsenic speciation without sample pretreatment is SPME. SPME has been largely applied to volatile compounds analysis in combination with GC and GC-MS, offering solvent-free and rapid sampling with low cost

and ease of operation; moreover, it is sensitive, selective and also compatible with low detection limits [84]. Especially, headspace solid phase micro extraction (HS-SPME) allows for the rapid fingerprinting of a plant's headspace [85-88], and HS sampling requires the optimization of the extraction parameters to be carried out. As has been previously reported in the literature, the most effective fibers from natural herbal matrices used are those consisting of three polymers: a liquid (PDMS) for the less polar components, and two solids, DVB and CAR, for the more polar components. Several conditions regarding the time and temperature for equilibrium and extraction have been reported, according the plant material analyzed [85-88]. To obtain a better understanding of the volatiles of chamomile, we investigated the chemical composition of chamomile essential oils extracted using HS-SPME/GC-MS with 65-μm polydimethylsiloxane/divinylbenzene (PDMS/DVB) fiber from the dried chamomile and compared to water extract, methanol extract and hexane layer from methanol extract of chamomile. In all cases, the analysis was carried out using gas chromatography (GC) and GC-MS.

Figure 10. Chamomile (*Matricaria recutita* L.)

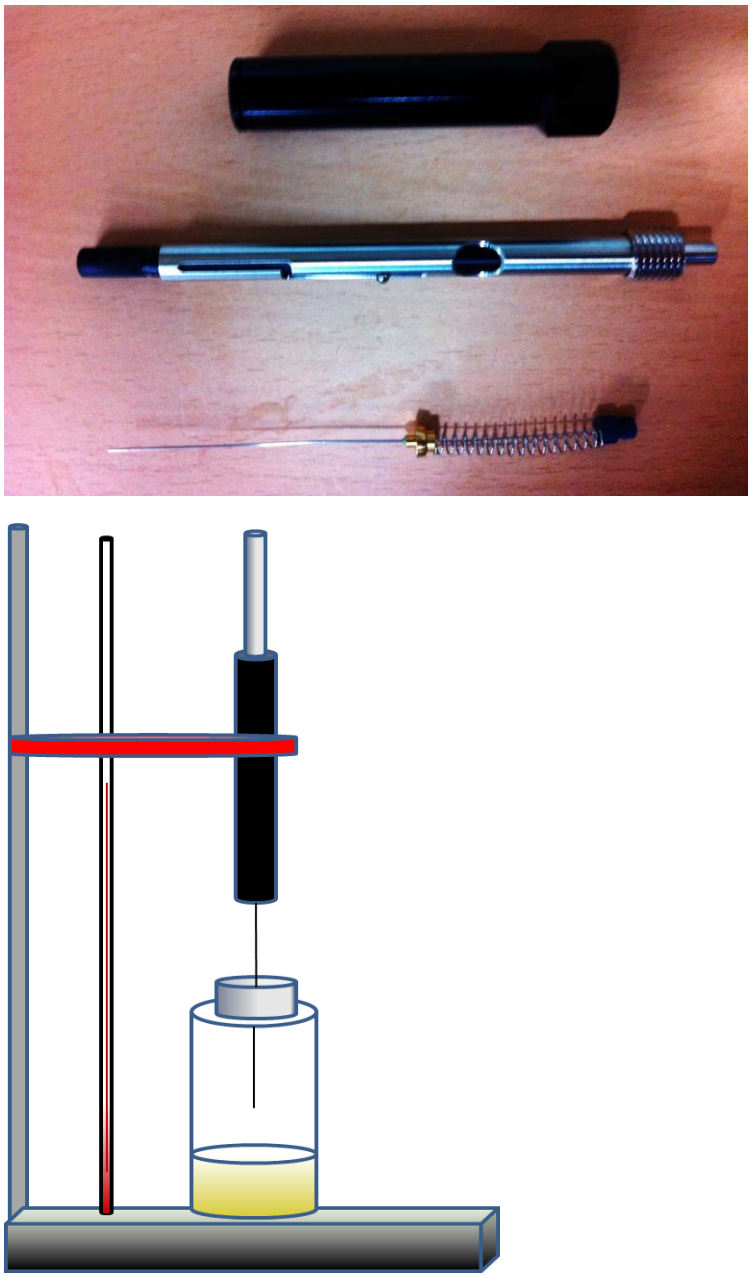

Figure 11. HS-SPME system

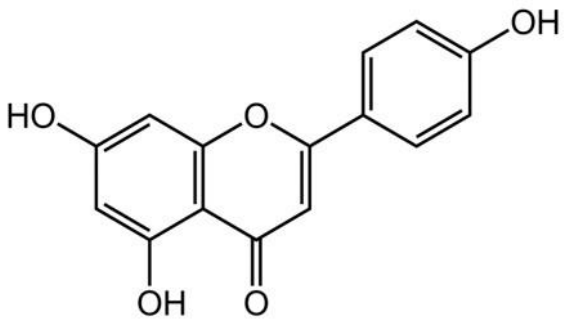

apigenin

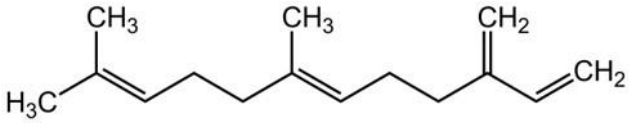

β-farnesene

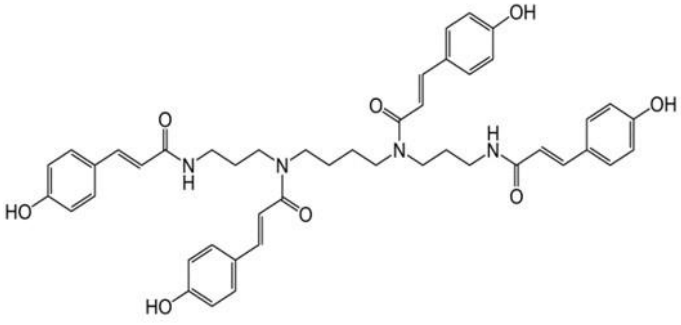

tetracoumaroyl spermine

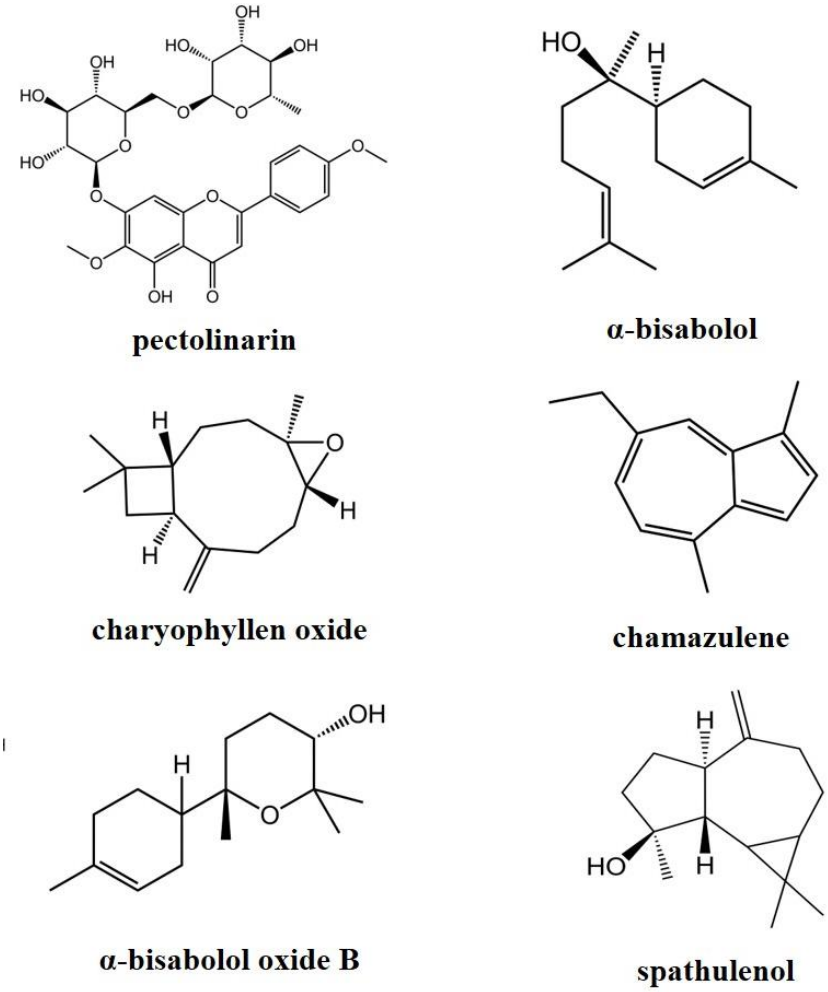

Figure 12. Chemical structures of major ingredients of chamomile

2. MATERIALS AND METHODS

2.1. Materials

2.1.1. Chemicals and reagents

DMEM culture medium, penicillin-streptomycin, D-PBS, trypan blue, DMSO, sulfanilamide, lipopolysaccharide (LPS), Tween 20, 4-methylumbelliferyl phosphate (4-MUP), HEPES, sodium bicarbonate and naphtylethylendiamine dihydrochloride were purchased from Sigma Chemical Co. Ltd (St. Louis, MO). FBS was purchased from South Pacific (New Zealand). PVDF membranes (Millipore, MA), Protein Assay Reagent (Bio-Rad, Vancouver, Canada), anti-iNOS, anti-COX-1, anti-COX-2, β-actin and horseradish peroxidase (HRP)-conjugated secondary antibody (Santa Cruz, CA, USA), ECL Plus detection kit (Amersham, UK) were used. All organic solvents used for column chromatography were of an analytical grade and purchased from Duksan pure chemical Co. in Korea. Phosphoric acid and methanol used for HPLC analysis and ESI-MS were of HPLC grade. Silica gel and diaion HP-20 resin (Mitsubishi chemicals, Co., Tokyo, Japan) were used for sample purification and the water was used distilled water. The SPME manual holder and the fiber of polydimethylsiloxane-divinylbenzene (PDMS-DVB, 65 μM) were purchased from Young-hwa science, Korea.

2.1.2. Sample preparation

German chamomile was obtained from Mt. Jiri in Korea. Five hundred grams of chamomile were boiled three times for 1 hr with 8 ℓ of methanol. The solvent was removed by rotary evaporation (N-1000s Eyela, Japan). The extract was lyophilized using a freeze dryer (FD5050, Ilshin Lab. Co. Ltd., Korea) and 118 g (yield (w/w) 23.0%) of crude extract was obtained. The dry extracts were DMSO before bioassay. For isolation of chamomile, 100 g of the crude extract was divided into four liquid-liquid partition fractions according to polarity; hexane, ethyl acetate, n-butanol, and water. These fractions were evaporated, freeze-dried and stored in a refrigerator prior to subsequent silica gel and diaion HP-20 column chromatography separation (Figure 13).

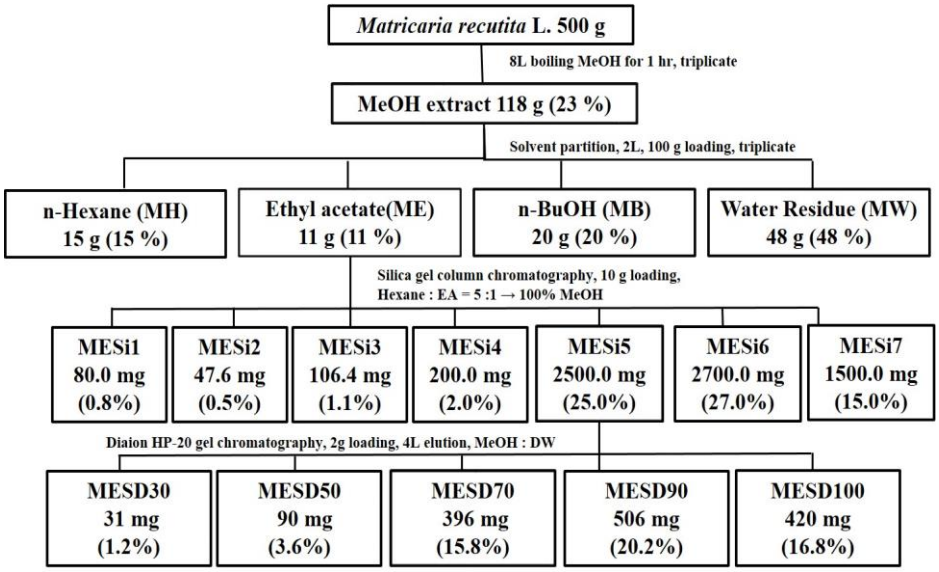

Figure 13. Schematic of the extraction and separation of German chamomile (*Matricaria recutita* L.)

2.1.3. Apparatus

CO_2 incubator, clean bench and plate centrifuge (Vision Scientific, Korea), centrifuge (Hanil Scientific, Korea), multiwell plate reader (Molecular Devices, Emax, Sunnyvale, CA, USA), multiwell plate fluorometer (Molecular Devices, Gemini XS, Sunnyvale, CA, USA) were used. The HPLC equipment used was consisted of L-6200A pump (Hitachi, Japan), a SIL-9A auto injector (Shimadzu, Japan), a TC-50 controller, a SEDEX 75 ELSD (SEDERE, France) and a Spectra 100 UV detector (Spectra-Physics, Mount View, CA, USA). Most reaction products were purified by column chromatography. Silica gel (particle size 60-200 μm) and diaion HP-20 resin (particle size 200-600 μm) were used for the column chromatography. ESI-MS experiments were conducted on an LCQ DECA XP ion-trap mass spectrometer (Thermo finnigan, San Jose, CA).

2.2. Methods

2.2.1. HS-SPME extraction

The fiber was conditioned by inserting them into the GC injector port according to the manufacture instructions before first use: 30 min at 250 °C for PDMS/DVB. Sample powders were quickly introduced into 20 mL headspace vials sealed with caps. The needle coated with fiber was inserted into the vials allowing the fibers exposed to the headspace above the samples.

After a period of extracting time at setting temperatures, the needle was removed from the headspace vials and directly inserted into the injection port of GC-MS. After a period of thermal desorption, the injected needle was removed and the GC-MS analysis procedure was initiated. Effects of different extracting temperature (40, 80 and 100 °C), extracting time (15, 30 and 45 min), sample amount (0.5, 1.0 and 1.5 g) and desorption time (1, 3 and 5 min) were investigated.

2.2.2. GC-MS analysis

GC-MS analyses were consisted of HP 5890 GC system and HP MD5790 mass spectrometer equipped with a single injector and flame ionization (FID). The apparatus was used for simultaneous sampling to HP-5MS capillary column (30 m x 0.25 mm, 0.25 μm). Temperature program: after at 70 °C for 5 min, 70 to 250 °C at 5 °C/min and then held isothermal 250 °C for 5 min. Carrier gas: high-purity helium (1 mL/min). Sample injection was conducted with a split-less mode. Injected volume was 0.1 μL. Ion source temperature: 150 °C; energy ionization: 70 eV; electron ionization mass spectra were acquired with a mass range of 35-350 Da.

2.2.3. Primary cell culture

Raw 264.7 cells, murine macrophages, were bought from American Type Culture Collection and suspended in DMEM with 10% FBS containing 100 U/mL of penicillin and 100 μg/mL of streptomycin. The cells were plated in a 75-cm2 tissue culture flask and stored in a 5% CO_2 humidified incubator (Vision scientific, Korea) at 37°C. For counting the cells, we used a hemocytometer and the number of viable cells was determined by trypan blue dye exclusion.

2.2.4. Cytotoxicity assay

For the cytotoxicity study, an MTT assay was used. In brief, RAW 264.7 cells were seeded 1.0×10^4 into each well of clear 96-wells pates with 100 μl of growth medium and incubated at 37 °C for 24 hr. They were supplied new culture medium and incubated with various concentrations of the samples for 24 hr. After incubation, the medium was changed to 100 μL of MTT solution for 2 h. Violet formazan was dissolved in DMSO for 15 min. The plates were then measured at 595 nm with a microplate reader (Emax, Molecular Devices, Sunnyvale, CA).

2.2.5. Assay for nitrite inhibition effect

The inhibitory effect on nitrite concentration by RAW 264.7 cells was

evaluated according to the Griess reagent. The cells were seeded in 24-well plates with 1×10^5 cells/well and incubated for 24 hr. After that the medium was replaced with the fresh medium containing various concentrations of samples and then 2 hr later LPS of 1 μg/mL was added into each well. After 18 hr, NO production was determined by measuring the accumulation of nitrite in the one hundred microliters of culture supernatant mixing with the same volume of Griess reagent (1% sulfanilamide in 5% phosphoric acid and 0.1% naphthylethylenediamine dihydrochloride in distilled water). The absorbance of the mixture was determined at 540 nm with a multiwell plate reader.

2.2.6. NF-κB SEAP reporter gene assay

The NF-κB SEAP inhibitory activity was determined in LPS-stimulated transfected-RAW 264.7 macrophages. The NF-κB-dependent reporter gene transcription was analyzed by the SEAP assay in accordance with previously described procedures [89]. 1×10^5 RAW 264.7 macrophages that were transfected with pNF-κB-SEAP-NPT, which encodes four copies of the –κB sequence and the SEAP gene as a reporter, were pre-incubated with different concentrations of each tested compound or the vehicle for 2 h and were then challenged with LPS (1 μg/mL) for an additional 16 h. TPCK (20 μM) was used as the positive control for this experiment.

2.2.7. Western blot analysis

Macrophage RAW 264.7 cells were seeded into 6 well plates at 1×10^6 cells/well and incubated for 24 h at 37 °C under 5% CO_2. The medium was replaced with fresh medium. Cells were pre-treated with sample for 2 hr and stimulated with LPS (1 μg/mL) for 18 hr. Cells were scrapped and washed three times with D-PBS and were lysed in 80 μL of lysis buffer (10 mM Tris-Cl, pH 7.4, 3 mM $CaCl_2$, 2 mM $MgCl_2$, 1% NP-40, 0.5 mM PMSF and protease inhibitor cocktail). The lysate was centrifuged at 13,500×g for 30 min and the supernatant was collected. The protein concentration was determined using the Bio-Rad Protein Assay Reagent (Bio-Rad, Hercules, CA). Cytoplasmic extracts were electrophoresed and then transferred onto PVDF membranes. After membrane was blocked by 5% skim milk for 1 h, membrane was incubated with primary antibody for 2 h, and then washed three times by TBST (a mixture of Tris-Buffered Saline and Tween 20) for 30 min. Membrane was further incubated with HRP-conjugated secondary antibody for 1 h. After washed three times for 30 min by TBST, the blot was developed for visualization by using the ECL Plus detection kit.

2.2.8. Statistical analysis

Values were expressed as the mean ± standard deviation (S.D.). The

statistical significance of the differences between the study groups was assessed by analysis of variance (ANOVA) followed by Student's t-test (SPSS version 10.0, Chicago, IL). The proportion of MTT, nitric oxide and NF-κB were measured in triplicate for each treatment on three separate occasions. Significance was assessed as $p < 0.05$ [$*p < 0.05$; $**p < 0.01$; $***p < 0.005$].

3. Results

3.1. Optimization of HS-SPME coupled to GC-MS for the chemical composition analysis of chamomile (*Matricaria recutita* L.)

3.1.1. Extraction profile obtained with different sample amount for six major compounds

Using different sample amounts of 0.5 g, 1.0 g and 1.5 g (dried chamomile powder), the peak intensity and quality was detected with GC-MS. For the six main components of chamomile, the extracted amount was greatest with 0.5 g sample amount (Figure 14A). Therefore, 0.5 g was found out to be the most optimal sample amount.

3.1.2. Extraction profile obtained with different extraction time for six major compounds

The extraction time of dried chamomile powders was set up at 15 min, 30 min and 45 min. For the six main components of chamomile, the extracted time was greatest with 30 min. Therefore, the 30 min was found out to be the most optimal extraction time (Figure 14B).

3.1.3. Extraction profile obtained with different extraction temperature for six major compounds

The extraction temperature of dried chamomile powders was set up at 40 °C, 80 °C and 100 °C. For the six main components of chamomile, the extracted temperature was greatest with 100 °C. Therefore, the 100 °C was found out to be the most optimal extraction temperature (Figure 14C).

3.1.4. Extraction profile obtained with different desorption time for six active compounds

The sample (1.0 g) was extracted with HS-SPME at 100°C for 30 minutes and then was subjected to GC-MS analysis. Using different times of desorption into the injector port, the peak profile was compared. When desorption time was set at 1 min, 3 min and 5 min, the intensity of peaks for six main components of chamomile was highest at 5 minute desorption time. Therefore, 5 minute was selected for desorption time (Figure 14D).

A

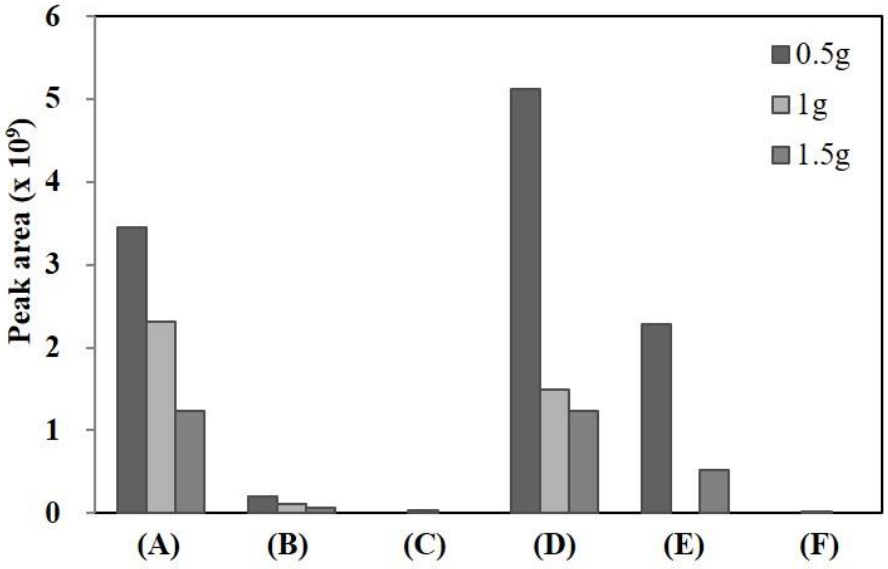
Peak area (x 10⁹)
6
5
4
3
2
1
0
0.5g
1g
1.5g
(A)
(B)
(C)
(D)
(E)
(F)

B

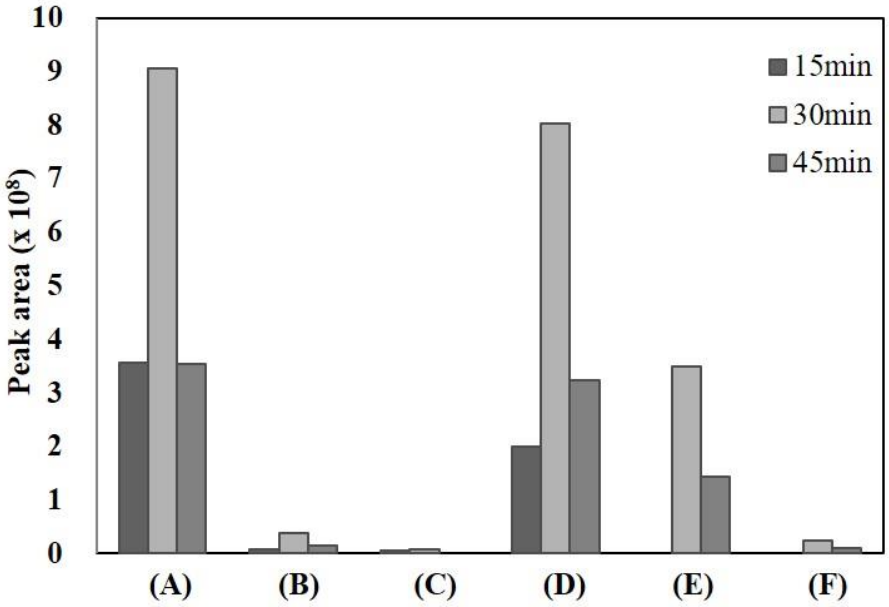
Peak area (x 10⁸)
10
9
8
7
6
5
4
3
2
1
0
15min
30min
45min
(A)
(B)
(C)
(D)
(E)
(F)

C

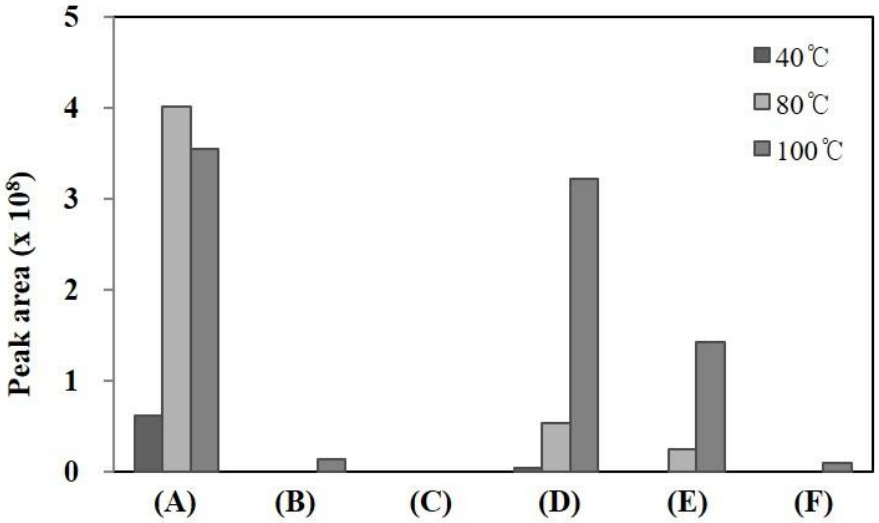
Peak area (x 10⁸)
5
4
3
2
1
0
40℃
80℃
100℃
(A)
(B)
(C)
(D)
(E)
(F)

D

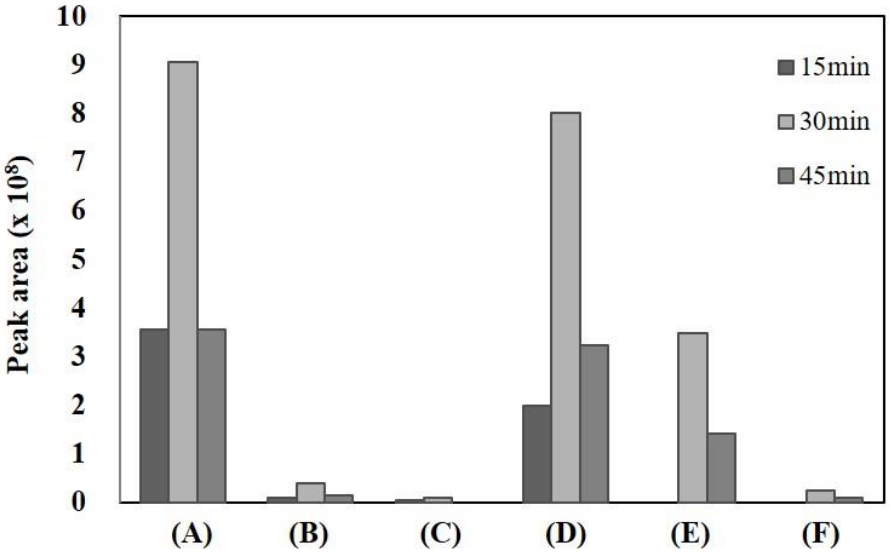
Peak area (x 10⁸)
10
9
8
7
6
5
4
3
2
1
0
15min
30min
45min
(A)
(B)
(C)
(D)
(E)
(F)

Figure 14. Extraction profile obtained with different analysis conditions for six active compounds in dried chamomile.

In order to determine extraction conditions, it was changed to sample amount, extraction time, extraction temperature and desorption time.

Selected extraction conditions: PDMS/DVB fiber, 0.5 g of dried chamomile powder, extraction time: 30min, extraction temperature: 100°C, desorption time: 5min; A - β-farnesene, B - spathulenol, C - caryophyllene oxide, D - α-bisabolol oxide B, E - α-bisabolol, F - chamazulene

3.1.5. SPME/GC-MS identification of chamomile volatiles and peak area percentage

Based on the results described above, the sample of 0.5 g was extracted at 100°C for 30 minutes and then was desorbed for 5 minutes on GC-MS system. Out of the total known number of 105 essential oil components in chamomile, 41 components were detected (Table 3). The component with the highest content in the sample was α-bisabolol oxide B (21.01%), followed by β-farnesene (17.89%) and α-bisabolol (9.04%). Chamazulene, which is a characteristic component of chamomile, but exists in extremely small amount and rarely detected in all chamomile plants, was detected and the content was 0.52% (MS quality: 97%).

Table 3. Essential oil components extracted by HS-SPME from dried chamomile at GC-MS

	Retention time (min)	Peak area (%)	MS quality (%)
β-pinene	5.68	0.17	90
eucalyptol	7.39	0.21	89
artemisia ketone	8.39	2.94	86
clorius (Niobe oil)	9.49	0.42	87
4,8-dimethyl-nona-3,8-dien-2-one	15.24	0.96	93
decanoic acid, methyl ester	16.72	0.52	97
dodecamethyl cyclohexasiloxane	16.89	0.08	91
1,4,6-trimethyl-1,2-dihydronaphthalene	17.46	0.36	95
eugenol	17.66	0.14	98
n-decanoic acid	18.51	2.26	95
γ-elemene	19.07	0.21	30
caryophyllene	19.42	0.57	96
β-farnesene	20.75	17.89	46
α-longipinene	21.12	0.33	93

	Retention time (min)	Peak area (%)	MS quality (%)
alloaromadendrene	21.30	0.23	91
γ-muurolene	21.39	0.98	99
bicyclogermacrene	21.59	0.43	95
α-farnesene	21.78	0.29	93
β-bisabolene	21.82	0.29	98
muurolene	22.01	0.14	99
δ-cadinene	22.26	0.43	97
2,4-dimethyl-qunoline	22.40	0.09	81
dihydroactinidiolide	22.46	0.11	95
cis-α-bisabolene	22.75	0.09	81
α-calacorene	22.82	0.07	93
trans-nerolidol	23.52	1.84	60
denderalasin	23.77	0.45	53
spathulenol	24.06	1.75	96
caryophyllene oxide	24.17	0.43	81
2-pinene	26.11	0.51	83

	Retention time (min)	Peak area (%)	MS quality (%)
α-bisabolol oxide B	27.36	21.01	58
brevifolin	27.71	0.62	93
α-bisabolol	28.31	9.04	43
chamazulene	29.91	0.52	97
(-)-kaurenoic acid	33.31	0.11	83
hexahydrofarnesyl acetone	35.80	0.20	60
2-(2,4-hexadiynylidene)-1,6-dioxaspiro(4.4)non-3-ene	38.20	1.59	90
palmitic acid, methyl ester	40.80	0.13	98
linolelaidic acid, methyl ester	47.98	0.06	99
linoleic acid, methyl ester	49.24	0.11	96
hexacosane	53.66	0.04	98

3.1.6. Comparison of the different extract composition obtained by SPME/GC-MS

Chamomile extracts of different solvents (water ex., ethanol ex., methanol ex. and hexane from methanol ex.) as well as the dried chamomile sample were subjected to HS-SPME and the composition of essential oils was analyzed by GC-MS. The data obtained with 100% water extract were compared with those obtained with 100% methanol extract because the profile of components extracted from 100% ethanol extract was same as that from 100% methanol extract (the comparison data are not included in this paper). The amount of extracted essential oils was less from water extract than from organic solvent extract. When compared to dried chamomile, both the water and organic solvent extracts contained remarkably less essential oil components in amount and in number of types and the MS quality was also low. α-bisabolol oxide B, which was shown to be present with highest content in chamomile, was detected in small amount and β-farnesene was not detected at all. Trans-nerolidol, spathulenol and chamazulene, which are azulenes, were not detected. The compound with highest content was herniarin and other compounds that had not been identified in dried chamomile or organic solvent extracts of chamomile such as cocoa hexenal and tetraglyme were detected. These compounds might have not been identified in the organic solvent extracts because the peak intensity was extremely low in the spectrum

of the organic solvent extracts. Meanwhile, the organic solvent extracts were shown to have high contents of α-bisabolol oxide B, β-farnesene and 2-(2,4-hexadiynylidene)-1,6-dioxaspiro(4,4)non-3-ene, demonstrating the profiles similar to the profile of dried chamomile sample. The hexane layer fractionated from the methanol extract (containing large amounts of essential oils) was subjected to SPME-GC-MS and was found to have very similar volatile essential oils to those identified in the methanol extract (Table 4).

Table 4. Essential oil components extracted by HS-SPME from water extract, methanol extract and hexane layer from chamomile methanol extract at GC-MS

Component name	Water Ex.		Methanol Ex.		Hexane layer	
	Area	MS quality (%)	Area	MS quality (%)	Area	MS quality (%)
artemisia ketone	0.11	50	-	-	-	-
7-methyl-1-naphthol	1.49	86	1.44	93	1.44	93
β-farnesene	-	-	5.16	98	5.16	98
4-(2,6,6-trimethylcyclohexa-1,3-di	2.17	96	-	-	-	-
cocoa hexenal	0.31	98	-	-	-	-
tetraglyme	0.28	83	-	-	-	-
(2E,4E)-5-chloro-3,4-dimethyl-2,4-	0.19	86	-	-	-	-
trans-nerolidol	-	-	0.64	90	0.64	90
spathulenol	-	-	1.59	97	-	-
α-bisabolol oxide B	1.22	83	21.73	95	21.73	95
herniarin	10.11	96	0.90	98	0.90	98
chamazulene	-	-	0.97	97	0.97	97

Component name	Water Ex.		Methanol Ex.		Hexane layer	
	Area	MS quality (%)	Area	MS quality (%)	Area	MS quality (%)
hexahydrofarnesyl acetone	-	-	0.50	91	0.50	91
2-(2,4-hexadiynylidene)-1,6-dioxaspiro(4.4)non-3-ene	3.71	87	12.38	90	12.38	90
palmitic acid, methyl ester	-	-	1.43	98	1.43	98
linolelaidic acid, methyl ester	-	-	0.71	99	0.71	99
11-octadecenoic acid, methyl ester					0.66	93
n-hexadecanoic acid	1.01	98	-	-	-	-
linoleic acid, methyl ester	-	-	0.50	90	0.50	90
octadecane	-	-	-	-	0.22	97

3.2. Bioactivity-guided isolation of anti-inflammatory active component from chamomile methanol extract

3.2.1. Inhibition of chamomile water, ethanol and methanol extract on cell viability, LPS-induced NO production and NF-κB SEAP activity

A nitrite assay using Griess reagent was conducted to determine whether the examined chamomile extracts produced an inhibitory effect on the production of NO after 18 h of LPS induction. All the chamomile extract have shown dose-dependent reductions in NO production. Macrophages RAW 264.7 harboring pNF-κB-SEAP-NPT construct [90], encoding four copies of κB sequence and SEAP gene as a reporter, were pretreated with each chamomile extract for 2 hr and stimulated with LPS (1 μg/mL) for 18 h. The cell-free culture media were heated at 65 °C for 5 min, and reacted with an assay buffer containing diethanolamine, MgCl2 and 4-methylumbelliferyl phosphate in the dark at room temperature for 1 hr. The level of NF- κB activation in transfected RAW 264.7 cells was tested using fluorescence method. All the chamomile extract also reduced LPS-stimulated NF-κB activation in a dose-dependent manner (Figure 15). Among them, the methanol extract has shown most potent activity for the suppression of NO production and NF-κB expression. The IC_{50} of water, ethanol and methanol extracts were 376.36 μg/mL, 139.90 μg/mL and 162.69 μg/mL for NO and

371.20 μg/mL, 358.12 μg/mL and 214.34 μg/mL for NF-κB, respectively.

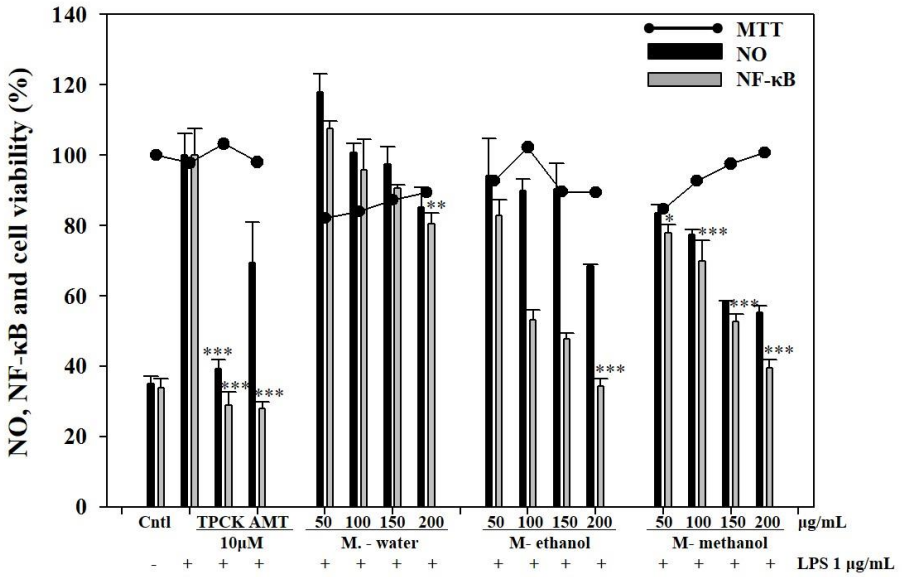

Figure 15. Effect on NO and NF-κB inhibition of various extracts from chamomile

Controls were excluded LPS or samples and were obtained from cells treated with 0.5% DMSO only. 10 μM AMT and 10 μM TPCK were used as positive controls for NO production and NF-κB expression, respectively. All of the experiments were performed in triplicate, and the results are represented as the mean ± S.D. Significance was assessed as $p < 0.05$ [*$p < 0.05$; **$p < 0.01$; ***$p < 0.005$]. Statistical analyses between LPS and crude extracts were performed using Student's *t*-test. LPS: lipopolysaccharide, DMSO: Dimethyl sulfoxide, AMT: 2-amino-5,6-dihydro-6-methyl-4H-1,-3-thiazine, TPCK: 2-N-p-tosyl-L-phenylalanine chloromethyl ketone, NO: nitric oxide

3.2.2. Inhibition of its liquid layers from chamomile methanol extract on cell viability, LPS-induced NO production and NF-κB SEAP activity

After solvent fractionation of chamomile, the MH (hexane-soluble layer), ME (ethyl acetate-soluble layer), MB (*n*-butanol-soluble layer) and MW (water-soluble layer) were obtained from the methanol extract. The inhibitory effects of four fractions from chamomile were compared on the production of Nitric oxide and NF-κB. AMT for NO and TPCK for NF-κB were used as a positive controls. As shown in Figure 16, ME significantly inhibited LPS-induced NO production in a dose-dependent manner without cytotoxicity.

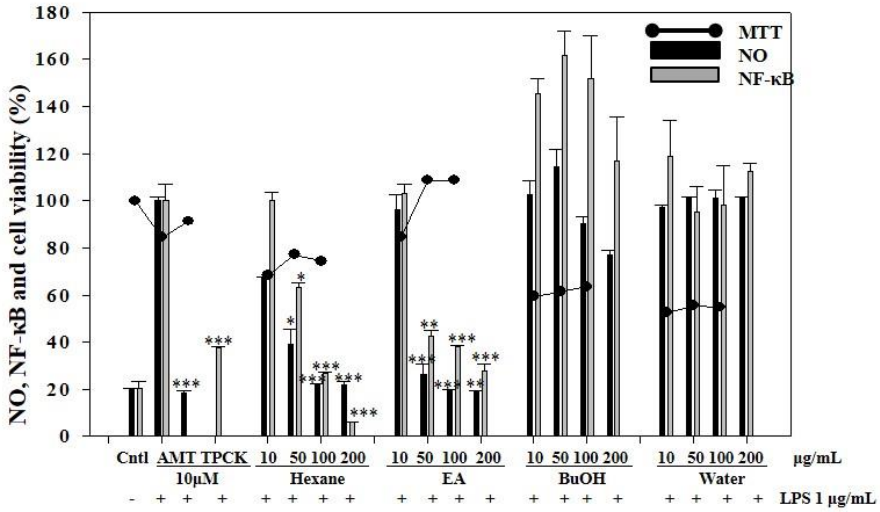

Figure 16. Effect on cell viability, NO production and NF-κB SEAP activity of different fractions from chamomile methanol extract

Controls were excluded LPS or samples and were obtained from cells treated with 0.5% DMSO only. 10 μM AMT and 10 μM TPCK were used as positive controls. All of the experiments were performed in triplicate, and the results are represented as the mean ± S.D. Significance was assessed as $p < 0.05$ [*$p < 0.05$; **$p < 0.01$; ***$p < 0.005$]. Statistical analyses between LPS and crude extracts were performed using Student's *t*-test.

3.2.3. Inhibition of fractions isolated by silica gel column chromatography from chamomile EA extract on cell viability and LPS-induced NO production and NF-κB SEAP activity

EA partition derived from methanol extract was further sub fractionated into seven fractions through silica gel column chromatography. Four fractions, which have lower polarity, have highly cytotoxicity and the 5^{th} to 7^{th} fractions have no cytotoxicity. Four less polar fractions have shown high cytotoxicity and 5^{th} to 7^{th} fractions have no cytotoxicity. Among these three fractions shown no cytotoxicity, 5^{th} fraction was the most powerful anti-inflammatory fraction inhibited the production of LPS-induced NO in a dose-dependent manner without any cytotoxicity. The IC_{50} of 5^{th} fraction was 20.6 μg/mL (Figure 17).

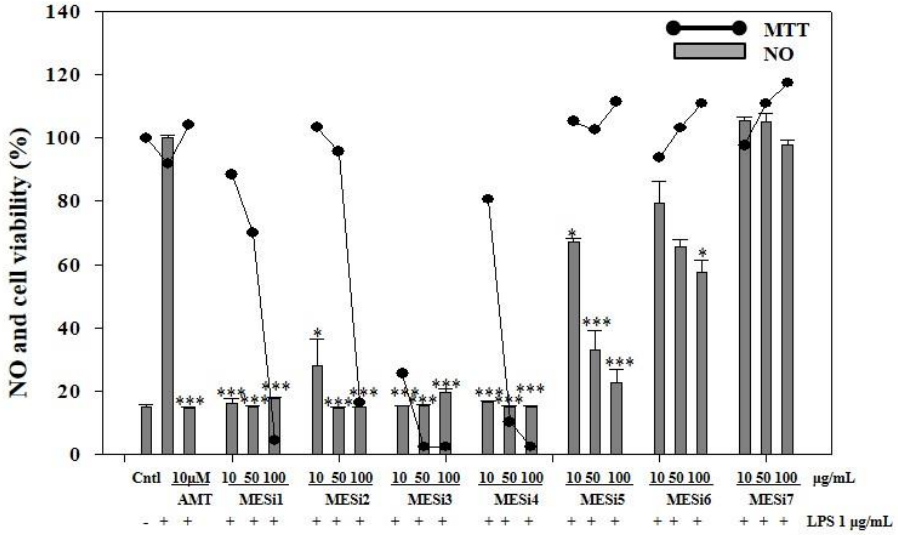

Figure 17. Effect on cell viability and NO production of different fractions from chamomile EA extract

Controls were excluded LPS or samples and were obtained from cells treated with 0.5% DMSO only. 10 μM AMT was used as positive controls. All of the experiments were performed in triplicate, and the results are represented as the mean ± S.D. Significance was assessed as $p < 0.05$ [*$p < 0.05$; **$p < 0.01$; ***$p < 0.005$]. Statistical analyses between LPS and crude extracts were performed using Student's t-test. MESi: Methanol extraction → Ethyl acetate layer → Silica gel chromatography

3.2.4. Inhibition of three enriched fractions isolated by Diaion HP-20 chromatography from 5th fraction by silica gel chromatography on cell viability and LPS-induced NO production

The 5th fraction derived from EA extract by silica gel column chromatography was isolated into five fractions through Diaion HP-20 column chromatography. Among those of five fractions, three component-enriched fractions were identified as dicaffeoyl quinic acid (eluted with 50% methanol, DCQ), apigenin-7-O-glucoside (eluted with 70% methanol, A7G) and tetracoumaroyl thermospermine (eluted with 90% methanol, TCTS). TCTS had the most potent inhibitory activity with an IC_{50} value of 7.5 μg/mL. IC_{50} values of DCQ and A7G were 173.7 μg/mL and 75.3 μg/mL, respectively (Figure 18).

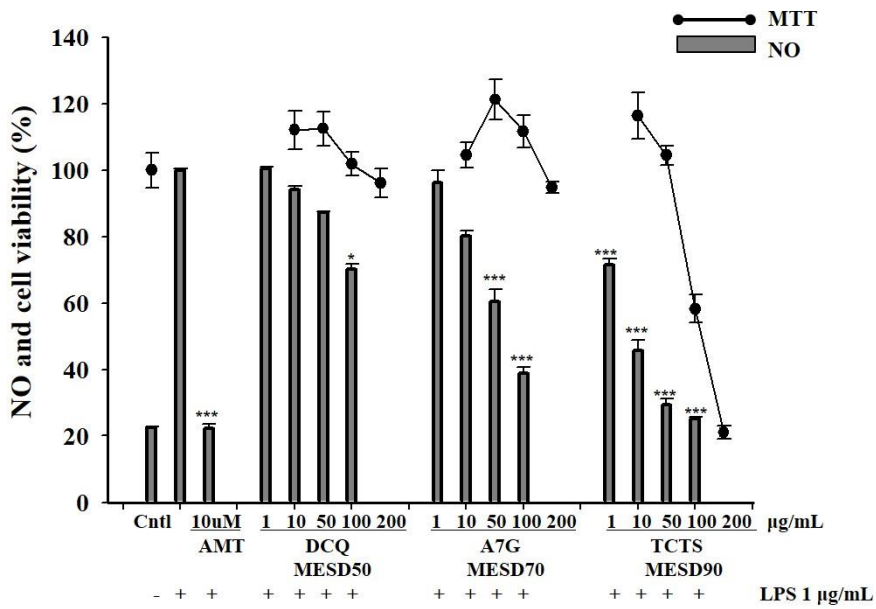

Figure 18. Effect on cell viability and NO production of different fractions from chamomile EA extract

Controls were excluded LPS or samples and were obtained from cells treated with 0.5% DMSO only. 10 μM AMT was used as positive controls. All of the experiments were performed in triplicate, and the results are represented as the mean ± S.D. Significance was assessed as $p < 0.05$ [*$p < 0.05$; **$p < 0.01$; ***$p < 0.005$]. Statistical analyses between LPS and crude extracts were performed using Student′s t-test. DCQ: dicaffeoyl-quinic acid enriched fraction, A7G: apigenin-7-O-glucoside enriched fraction, TCTS: tetracoumaroyl thermospermine enriched fraction

3.2.5. Inhibition of three enriched fractions isolated by Diaion HP-20 chromatography from 5th fraction by silica gel chromatography on the protein levels of COX-1, COX-2, and iNOS in LPS stimulated RAW 264.7 macrophages

The protein expressions of iNOS, COX-1, and COX-2 were also examined in LPS-stimulated RAW 264.7 cells that had been treated with one of the three enriched fractions that were isolated from chamomile by diaion HP-20 chromatography in Figure 19. The results from this assessment demonstrated that A7G and TCTS enriched fractions diminished the protein levels of both iNOS and COX-2. TCTS had the most potent inhibitory effect on iNOS and COX-2.

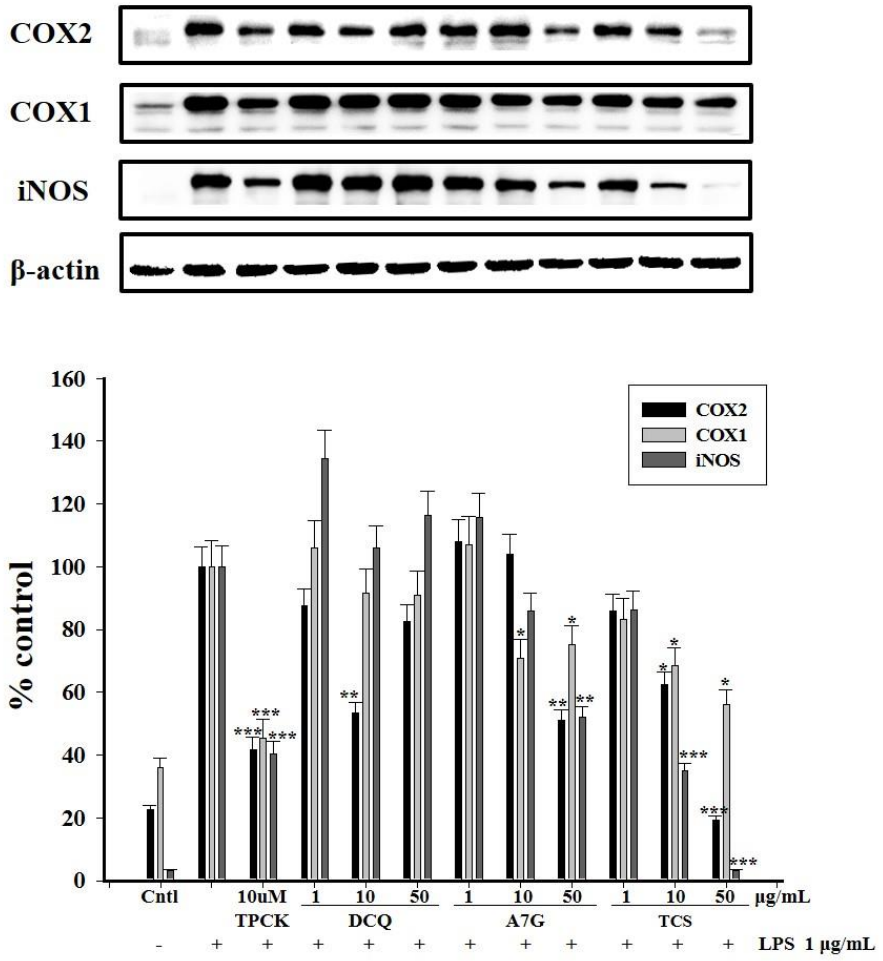

Figure 19. Effect of three enriched fractions from chamomile on the protein levels of iNOS, COX-1, and COX-2 in LPS-induced RAW 264.7 macrophages

The cells were treated with DCQ, A7G, and TCTS enriched fractions (1, 10 and 50 μg/mL) and LPS (1 μg/mL) for 20 hr. The expression levels of the iNOS, COX-1, COX-2, and β-actin were detected using specific antibodies. In this experiment, 10 μM TPCK was used as positive control. All of the

experiments were performed in triplicate. DCQ: Dicaffeoyl-quinic acid enriched fraction, A7G: Apigenin-7-O-glucoside enriched fraction, TCTS: tetracoumaroyl thermospermine enriched fraction

3.2.6. Inhibition of tetra-coumaroyl thermospermine enriched fractions on the protein levels of ERK, Akt, and STAT3 in LPS stimulated RAW 264.7 macrophages

In order to figure out the reason for the inhibitory activity of NO production, NF-κB activation and the expressions of iNOS and COX-2 protein, signaling pathway was checked using Western blot analysis. Upon LPS challenge, the protein expression levels of ERK, Akt, and STAT3 are dramatically decreased at 50 μg/mL of TCTS due to their phosphorylation, in particular, TCTS dose dependently inhibited phosphorylation of STAT3 signals.

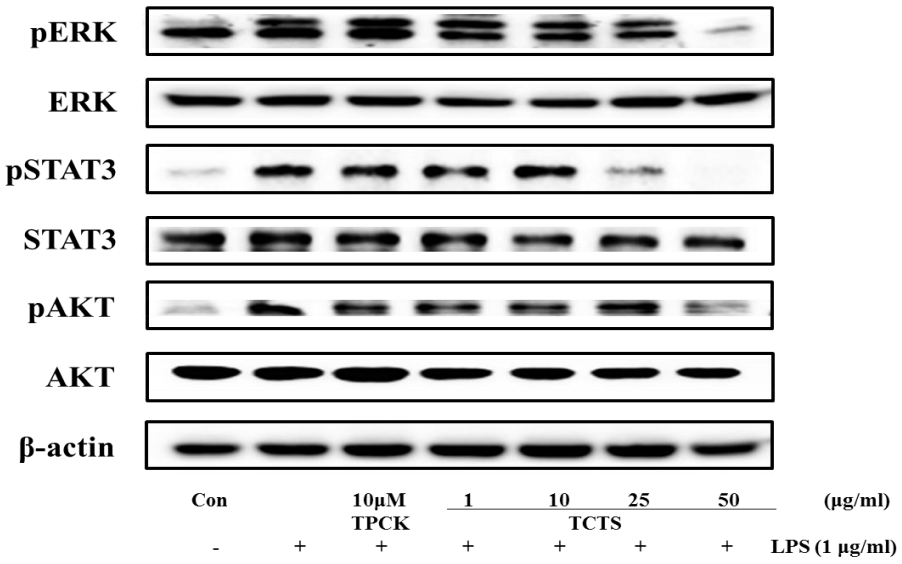

Figure 20. Effect of TCTS on the ERK, Akt, and STAT3 pathways

The levels of phosphorylated ERK, Akt, and STAT3 proteins in total protein extracts were determined by Western blot analysis using specific antibodies. In this experiment, 10 μM TPCK was used as positive control. All of the experiments were performed in triplicate. TCTS: tetracoumaroyl thermospermine enriched fraction

4. Discussion

Chamomile is known to possess anti-inflammatory and anti-oxidant effects. In the present study, water, ethanol and methanol extracts of dried chamomile were each assayed for anti-inflammatory activity. The assay showed a dose-dependent inhibition in all of the extracts and a higher inhibition in the organic solvent extracts than in the water extract. Methanol is less polar than water and therefore the methanol extract contains more essential oils than the water extract. Therefore, the chemical component analysis was performed with the methanol extract of chamomile to identify essential oil components contained in the methanol extract of chamomile.

The HS-SPME was selected as an extraction method because it allows the extraction of trace amount of essential oil components in chamomile, but the most optimal conditions for the extraction of chamomile samples to be used in the study needed to be established. In order to find out the optimal conditions for detecting major essential oil components of chamomile, i.e., β-farnesene, spathulenol, caryophyllene oxide, α-bisabolol oxide B, α-bisabolol and chamazulene, the chamomile samples were analyzed using different conditions of sample amount, extraction time, extraction temperature and desorption time on GC-MS. The most optimal condition for extraction was found to be 0.5 mg of sample amount, 30 minutes of extraction time, 100°C of extraction temperature and 5 minutes of desorption time. Using the most

optimal condition identified, 41 out of the total known number of 105 essential oil components in chamomile including major components could be identified in the dried chamomile sample. The same conditions as above for HS-SPME coupled to GC-MS were used to identify essential oil components contained in 100% water extract of chamomile, 100% methanol extract of chamomile and hexane layer from the methanol extract of chamomile, respectively. The GC-MS profiles showed that the water extract contained remarkably less essential oil components both in amount and in number of types than the organic solvent extracts and the MS quality of the water extract was also low. The water extract of chamomile was shown to contain small amount of α-bisabolol oxide B, which was present with high content in dried chamomile, but major active components such as β-farnesene, trans-nerolidol, spathulenol and chamazulene were not identified. The compound with highest content was herniarin and other compounds that had not been identified in dried chamomile or organic solvent extracts of chamomile such as cocoa hexenal and tetraglyme were detected. These compounds might have not been identified in the organic solvent extracts because the peak intensity was extremely low in the gas chromatogram of the organic solvent extracts. Meanwhile, the organic solvent extracts were shown to have large amounts of α-bisabolol oxide B and 2-(2,4-Hexadiynylidene)-1,6-dioxaspiro(4,4)non-3-ene, demonstrating the profiles similar to that of non-extracted dried

chamomile sample. The compounds identified in the hexane layer fractionated from the methanol extract (the liquid layer containing large amounts of essential oils) were found to be very similar to the volatile essential oils identified in the methanol extract. Based on the identification of essential oil components, the organic solvent extracts containing large amounts of essential oil components are thought to have a higher anti-inflammatory effect. Therefore, the methanol extract of chamomile was analyzed to identify anti-inflammatory compounds. Fractionation using liquid-liquid separation was performed to identify non-volatile active compounds as well. The methanol extract of chamomile was fractionated into hexane, EA, BuOH, and water layers.

The less polar hexane and EA-soluble layers were shown, as expected, to have higher inhibitory effects on NO generation and NF-κB expression, but the hexane layer was also found to have toxicity. Therefore, the EA layer containing large amount of flavonoids was selected for further separation. The EA layer was separated into seven fractions by silica gel column chromatography. Of those seven fractions, 2^{nd} and 5^{th} fractions were found to have IC_{50} values of 5.34 μg/mL and 20.60 μg/mL, respectively. The 2^{nd} fraction was ruled out because of its extremely high toxicity and the 5^{th} fraction with no toxicity and high yield was selected to be further separated. In the next step, the 5^{th} fraction was separated into a total of 5 fractions using

Diaion HP-20 column chromatography. From those fractions, three main components - dicaffeoyl quinic acids enriched (50% MeOH, DCQ), apigenin 7-O-glucoside derivatives enriched (70% MeOH, A7G) and tetracoumaroyl thermospermine enriched (90% MeOH, TCTS) – were identified, among which TCTS was shown to have the highest NO inhibition effect. Within the range of concentrations at which no toxicity was observed, TCTS was assayed for the iNOS, COX-1, and COX-2 expressions of proteins associated with inflammation using Western blot analysis. TCTS was shown to have higher inhibitory effects on the expression of iNOS and COX-2 proteins compared to DCQ and A7G. The selective inhibition effect on COX-2 has previously been reported with chamomile [91], but the active compound was not identified. In this study, it was also found that the COX-2 inhibition of TCTS was exerted via ERK/Akt and STAT3 pathway.

Chamomile is known to have anti-inflammatory, anti-cancer and sedative effects [92, 93]. The studies to identify anti-cancer components of chamomile have already been conducted, but no studies to separate and identify anti-inflammatory components of chamomile have yet been undertaken. Therefore, this study also included the bioactivity-guided isolation for the identification of essential oil components or other active compounds responsible for chamomile's anti-inflammatory effect. The result showed that the dried chamomile contained large amounts of anti-inflammatory compounds such as

α-bisabolol oxide B, β-farnesene and α-bisabolol. The higher anti-inflammatory effect shown in the methanol extract than in the water extract was deemed to be due to the greater amount of essential oil components contained in the methanol extract. The bioactivity-guided isolation performed to explore non-volatile active components showed that TCTS is mainly responsible for the anti-inflammatory effect of chamomile with COX-2 inhibition via ERK/Akt and STAT3 pathway.

5. References

[1] B.B. Aggarwal, Targeting inflammation-induced obesity and metabolic diseases by curcumin and other nutraceuticals, Annual review of nutrition, 30 (2010) 173-199.

[2] G.A. Bray, A concise review on the therapeutics of obesity, Nutrition, 16 (2000) 953-960.

[3] F.L. Greenway, S.R. Smith, The future of obesity research, Nutrition, 16 (2000) 976-982.

[4] E.S. Idogun, E.I. Unuigbe, A.A. Famodu, O.T. Akinola, Body mass index in type 2 diabetes mellitus complications: hypertensive diabetics and diabetic nephropathy, The Nigerian postgraduate medical journal, 13 (2006) 17-20.

[5] J. Blundell, Pharmacological approaches to appetite suppression, Trends in pharmacological sciences, 12 (1991) 147-157.

[6] C.A. Baile, J.Y. Yang, S. Rayalam, D.L. Hartzell, C.Y. Lai, C. Andersen, M.A. Della-Fera, Effect of resveratrol on fat mobilization, Annals of the New York Academy of Sciences, 1215 (2011) 40-47.

[7] G. de Simone, G. D'Addeo, Sibutramine: balancing weight loss benefit and possible cardiovascular risk, Nutrition, metabolism, and cardiovascular diseases : NMCD, 18 (2008) 337-341.

[8] L. Karamadoukis, G.H. Shivashankar, L. Ludeman, A.J. Williams, An unusual complication of treatment with orlistat, Clinical nephrology, 71 (2009) 430-432.

[9] L. Slovacek, V. Pavlik, B. Slovackova, The effect of sibutramine therapy on occurrence of depression symptoms among obese patients, Nutrition, metabolism, and cardiovascular diseases : NMCD, 18 (2008) e43-44.

[10] P.H. Thurairajah, W.K. Syn, D.A. Neil, D. Stell, G. Haydon, Orlistat (Xenical)-induced subacute liver failure, European journal of gastroenterology & hepatology, 17 (2005) 1437-1438.

[11] M. O'Hara, D. Kiefer, K. Farrell, K. Kemper, A review of 12 commonly used medicinal herbs, Arch Fam Med, 7 (1998) 523-536.

[12] N. Hasegawa, N. Yamda, M. Mori, Powdered green tea has antilipogenic effect on Zucker rats fed a high-fat diet, Phytother Res, 17 (2003) 477-480.

[13] A. Elkayam, D. Mirelman, E. Peleg, M. Wilchek, T. Miron, A. Rabinkov, M. Oron-Herman, T. Rosenthal, The effects of allicin on weight in fructose-induced hyperinsulinemic, hyperlipidemic, hypertensive rats, Am J Hypertens, 16 (2003) 1053-1056.

[14] K.M. Hargrave, C.L. Li, B.J. Meyer, S.D. Kachman, D.L. Hartzell, M.A. Della-Fera, J.L. Miner, C.A. Baile, Adipose depletion and apoptosis induced by trans-10, cis-12 conjugated linoleic acid in mice, Obes Res, 10 (2002) 1284-1290.

[15] F. Thielecke, M. Boschmann, The potential role of green tea catechins in the prevention of the metabolic syndrome - a review, Phytochemistry, 70 (2009) 11-24.

[16] S. Wolfram, Y. Wang, F. Thielecke, Anti-obesity effects of green tea: from bedside to bench, Molecular nutrition & food research, 50 (2006) 176-187.

[17] S. Rayalam, M.A. Della-Fera, C.A. Baile, Phytochemicals and regulation of the adipocyte life cycle, The Journal of nutritional biochemistry, 19 (2008) 717-726.

[18] O.A. MacDougald, M.D. Lane, Transcriptional regulation of gene expression during adipocyte differentiation, Annu Rev Biochem, 64 (1995) 345-373.

[19] I. Shimomura, R.E. Hammer, J.A. Richardson, S. Ikemoto, Y. Bashmakov, J.L. Goldstein, M.S. Brown, Insulin resistance and diabetes mellitus in transgenic mice expressing nuclear SREBP-1c in adipose tissue: model for congenital generalized lipodystrophy, Genes Dev, 12 (1998) 3182-3194.

[20] H. Green, M. Meuth, An established pre-adipose cell line and its differentiation in culture, Cell, 3 (1974) 127-133.

[21] H. Green, O. Kehinde, An established preadipose cell line and its differentiation in culture. II. Factors affecting the adipose conversion,

Cell, 5 (1975) 19-27.

[22] A.K. Hindle, J. Koury, T. McCaffrey, S.W. Fu, F. Brody, Dysregulation of gene expression within the peroxisome proliferator activated receptor pathway in morbidly obese patients, Surg Endosc, 23 (2009) 1292-1297.

[23] P. Tontonoz, E. Hu, R.A. Graves, A.I. Budavari, B.M. Spiegelman, mPPAR gamma 2: tissue-specific regulator of an adipocyte enhancer, Genes Dev, 8 (1994) 1224-1234.

[24] J.M. Corton, J.G. Gillespie, D.G. Hardie, Role of the AMP-activated protein kinase in the cellular stress response, Curr Biol, 4 (1994) 315-324.

[25] M. Rossmeisl, P. Flachs, P. Brauner, J. Sponarova, O. Matejkova, T. Prazak, J. Ruzickova, K. Bardova, O. Kuda, J. Kopecky, Role of energy charge and AMP-activated protein kinase in adipocytes in the control of body fat stores, Int J Obes Relat Metab Disord, 28 Suppl 4 (2004) S38-44.

[26] J. Sponarova, K.J. Mustard, O. Horakova, P. Flachs, M. Rossmeisl, P. Brauner, K. Bardova, M. Thomason-Hughes, R. Braunerova, P. Janovska, D.G. Hardie, J. Kopecky, Involvement of AMP-activated protein kinase in fat depot-specific metabolic changes during starvation, FEBS Lett, 579 (2005) 6105-6110.

[27] J.B. Prins, S. O'Rahilly, Regulation of adipose cell number in man, Clin Sci (Lond), 92 (1997) 3-11.

[28] A. Sorisky, R. Magun, A.M. Gagnon, Adipose cell apoptosis: death in the energy depot, Int J Obes Relat Metab Disord, 24 Suppl 4 (2000) S3-7.

[29] W. Yin, J. Mu, M.J. Birnbaum, Role of AMP-activated protein kinase in cyclic AMP-dependent lipolysis In 3T3-L1 adipocytes, J Biol Chem, 278 (2003) 43074-43080.

[30] M. Daval, F. Diot-Dupuy, R. Bazin, I. Hainault, B. Viollet, S. Vaulont, E. Hajduch, P. Ferre, F. Foufelle, Anti-lipolytic action of AMP-activated protein kinase in rodent adipocytes, J Biol Chem, 280 (2005) 25250-25257.

[31] J.B. Prins, N.I. Walker, C.M. Winterford, D.P. Cameron, Human

adipocyte apoptosis occurs in malignancy, Biochemical and biophysical research communications, 205 (1994) 625-630.

[32] J.B. Prins, C.U. Niesler, C.M. Winterford, N.A. Bright, K. Siddle, S. O'Rahilly, N.I. Walker, D.P. Cameron, Tumor necrosis factor-alpha induces apoptosis of human adipose cells, Diabetes, 46 (1997) 1939-1944.

[33] W.H. Miller, Jr., I.M. Faust, A.C. Goldberger, J. Hirsch, Effects of severe long-term food deprivation and refeeding on adipose tissue cells in the rat, Am J Physiol, 245 (1983) E74-80.

[34] H. Qian, M.J. Azain, M.M. Compton, D.L. Hartzell, G.J. Hausman, C.A. Baile, Brain administration of leptin causes deletion of adipocytes by apoptosis, Endocrinology, 139 (1998) 791-794.

[35] T. Adachi, T. Toishi, H. Wu, T. Kamiya, H. Hara, Expression of extracellular superoxide dismutase during adipose differentiation in 3T3-L1 cells, Redox Rep, 14 (2009) 34-40.

[36] S. Furukawa, T. Fujita, M. Shimabukuro, M. Iwaki, Y. Yamada, Y. Nakajima, O. Nakayama, M. Makishima, M. Matsuda, I. Shimomura, Increased oxidative stress in obesity and its impact on metabolic syndrome, J Clin Invest, 114 (2004) 1752-1761.

[37] H.K. Vincent, A.G. Taylor, Biomarkers and potential mechanisms of obesity-induced oxidant stress in humans, Int J Obes (Lond), 30 (2006) 400-418.

[38] Q.Y. Zhang, G.Z. Tu, Y.Y. Zhao, T.M. Cheng, Novel bioactive isoquinoline alkaloids from *Carduus crispus*, Tetrahedron, 58 (2002) 6795-6798.

[39] D.M. Jeong, H.A. Jung, J.S. Choi, Comparative antioxidant activity and HPLC profiles of some selected Korean thistles, Archives of pharmacal research, 31 (2008) 28-33.

[40] E.J. Lee, E.J. Joo, Y.N. Hong, Y.S. Kim, Inhibition of adipocyte differentiation by MeOH Extract from *Carduus crispus* through ERK and p38 MAPK pathways, Natural Product Sciences 17 (2011) 273-278.

[41] K.D. Flora, H.R. Rosen, K.G. Benner, The use of naturopathic remedies

for chronic liver disease, Am J Gastroenterol, 91 (1996) 2654-2655.

[42] S. Liu, X. Luo, D. Li, J. Zhang, D. Qiu, W. Liu, L. She, Z. Yang, Tumor inhibition and improved immunity in mice treated with flavone from Cirsium japonicum DC, Int Immunopharmacol, 6 (2006) 1387-1393.

[43] Y. Ito, Countercurrent chromatography, J Biochem Biophys Methods, 5 (1981) 105-129.

[44] M. Zhao, Y. Ito, P. Tu, Isolation of a novel flavanone 6-glucoside from the flowers of Carthamus tinctorium (Honghua) by high-speed counter-current chromatography, J Chromatogr A, 1090 (2005) 193-196.

[45] X. Ma, T. Zhang, Y. Wei, P. Tu, Y. Chen, Y. Ito, Preparative isolation and purification of calycosin from Astragalus membranaceus Bge. var. mongholicus (Bge.) Hsiao by high-speed counter-current chromatography, J Chromatogr A, 962 (2002) 243-247.

[46] X. Ma, P. Tu, Y. Chen, T. Zhang, Y. Wei, Y. Ito, Preparative isolation and purification of two isoflavones from Astragalus membranaceus Bge. var. mongholicus (Bge.) Hsiao by high-speed counter-current chromatography, J Chromatogr A, 992 (2003) 193-197.

[47] X. Ma, P. Tu, Y. Chen, T. Zhang, Y. Wei, Y. Ito, Preparative isolation and purification of isoflavan and pterocarpan glycosides from Astragalus membranaceus Bge. var. mongholicus (Bge.) Hsiao by high-speed counter-current chromatography, J Chromatogr A, 1023 (2004) 311-315.

[48] L. Lei, F. Yang, T. Zhang, P. Tu, L. Wu, Y. Ito, Preparative isolation and purification of acteoside and 2'-acetyl acteoside from Cistanches salsa (C.A. Mey.) G. Beck by high-speed counter-current chromatography, J Chromatogr A, 912 (2001) 181-185.

[49] W. Jin, P.F. Tu, Preparative isolation and purification of trans-3,5,4'-trihydroxystilbene-4'-O-beta-D-glucopyranoside and (+)catechin from Rheum tanguticum Maxim. ex Balf. using high-speed counter-current chromatography by stepwise elution and stepwise increasing the flow-rate of the mobile phase, J Chromatogr A, 1092 (2005) 241-245.

[50] K.L. Wolfe, R.H. Liu, Cellular antioxidant activity (CAA) assay for assessing antioxidants, foods, and dietary supplements, J Agric Food

Chem, 55 (2007) 8896-8907.

[51] O.A. Eldahshan, Isolation and structure elucidation of phenolic compounds of Carob leaves grown in Egypt, Current Research Journal of Biological Sciences, 3 (2011) 52-55.

[52] E.D. Rosen, C.H. Hsu, X. Wang, S. Sakai, M.W. Freeman, F.J. Gonzalez, B.M. Spiegelman, C/EBPalpha induces adipogenesis through PPARgamma: a unified pathway, Genes & development, 16 (2002) 22-26.

[53] P. Tontonoz, E. Hu, B.M. Spiegelman, Stimulation of adipogenesis in fibroblasts by PPAR gamma 2, a lipid-activated transcription factor, Cell, 79 (1994) 1147-1156.

[54] J.M. Ntambi, K. Young-Cheul, Adipocyte differentiation and gene expression, The Journal of nutrition, 130 (2000) 3122S-3126S.

[55] O. Bezy, C. Vernochet, S. Gesta, S.R. Farmer, C.R. Kahn, TRB3 blocks adipocyte differentiation through the inhibition of C/EBPbeta transcriptional activity, Molecular and cellular biology, 27 (2007) 6818-6831.

[56] Y. Dagon, Y. Avraham, E.M. Berry, AMPK activation regulates apoptosis, adipogenesis, and lipolysis by eIF2alpha in adipocytes, Biochemical and biophysical research communications, 340 (2006) 43-47.

[57] S. Shukla, S. Gupta, Apigenin: a promising molecule for cancer prevention, Pharmaceutical research, 27 (2010) 962-978.

[58] D.L. McKay, J.B. Blumberg, A review of the bioactivity and potential health benefits of chamomile tea *(Matricaria recutita* L.), Phytother Res, 20 (2006) 519-530.

[59] S. Shukla, S. Gupta, Suppression of constitutive and tumor necrosis factor alpha-induced nuclear factor (NF)-kappaB activation and induction of apoptosis by apigenin in human prostate carcinoma PC-3 cells: correlation with down-regulation of NF-kappaB-responsive genes, Clinical cancer research : an official journal of the American Association for Cancer Research, 10 (2004) 3169-3178.

[60] C. Wang, M.S. Kurzer, Phytoestrogen concentration determines effects

on DNA synthesis in human breast cancer cells, Nutrition and cancer, 28 (1997) 236-247.

[61] W. Wang, L. Heideman, C.S. Chung, J.C. Pelling, K.J. Koehler, D.F. Birt, Cell-cycle arrest at G2/M and growth inhibition by apigenin in human colon carcinoma cell lines, Molecular carcinogenesis, 28 (2000) 102-110.

[62] M. Feldmann, R.N. Maini, The role of cytokines in the pathogenesis of rheumatoid arthritis, Rheumatology (Oxford), 38 Suppl 2 (1999) 3-7.

[63] T.A. Libermann, D. Baltimore, Activation of interleukin-6 gene expression through the NF-kappa B transcription factor, Mol Cell Biol, 10 (1990) 2327-2334.

[64] D.L. McKay, J.B. Blumberg, A review of the bioactivity and potential health benefits of peppermint tea (Mentha piperita L.), Phytother Res, 20 (2006) 619-633.

[65] P. Gardiner, Complementary, holistic, and integrative medicine: chamomile, Pediatr Rev, 28 (2007) e16-18.

[66] M. Ganzera, P. Schneider, H. Stuppner, Inhibitory effects of the essential oil of chamomile (Matricaria recutita L.) and its major constituents on human cytochrome P450 enzymes, Life Sci, 78 (2006) 856-861.

[67] V. Svehlikova, R.N. Bennett, F.A. Mellon, P.W. Needs, S. Piacente, P.A. Kroon, Y. Bao, Isolation, identification and stability of acylated derivatives of apigenin 7-O-glucoside from chamomile (Chamomilla recutita [L.] Rauschert), Phytochemistry, 65 (2004) 2323-2332.

[68] R. Avallone, P. Zanoli, G. Puia, M. Kleinschnitz, P. Schreier, M. Baraldi, Pharmacological profile of apigenin, a flavonoid isolated from Matricaria chamomilla, Biochem Pharmacol, 59 (2000) 1387-1394.

[69] V.E. Tyler, V.E. Tyler, The honest herbal : a sensible guide to the use of herbs and related remedies, 3rd ed., Pharmaceutical Products Press, New York, 1992.

[70] H.B. Forster, H. Niklas, S. Lutz, Antispasmodic effects of some medicinal plants, Planta Med, 40 (1980) 309-319.

[71] K.G. Lee, T. Shibamoto, Determination of antioxidant potential of volatile extracts isolated from various herbs and spices, J Agric Food

Chem, 50 (2002) 4947-4952.

[72] N.O. Babenko, O.H. Shakhova, [Age-dependent effects of flavonoids on secretory function of the rat liver], Fiziol Zh, 51 (2005) 65-69.

[73] C. Di Giorgio, F. Delmas, M. Tueni, E. Cheble, T. Khalil, G. Balansard, Alternative and complementary antileishmanial treatments: assessment of the antileishmanial activity of 27 Lebanese plants, including 11 endemic species, J Altern Complement Med, 14 (2008) 157-162.

[74] G.R. Skovgaard, A.S. Jensen, M.L. Sigler, Effect of a novel dietary supplement on skin aging in post-menopausal women, Eur J Clin Nutr, 60 (2006) 1201-1206.

[75] G. Buchbauer, C.T. Klein, B. Wailzer, P. Wolschann, Threshold-based structure-activity relationships of pyrazines with bell-pepper flavor, J Agric Food Chem, 48 (2000) 4273-4278.

[76] G. Buchbauer, L. Jirovetz, W. Jager, C. Plank, H. Dietrich, Fragrance compounds and essential oils with sedative effects upon inhalation, J Pharm Sci, 82 (1993) 660-664.

[77] L. Coiffard, M. Piron-Frenet, L. Amicel, Geographical variations of the constituents of the essential oil of Crithmum maritimum L., Apiaceae, Int J Cosmet Sci, 15 (1993) 15-21.

[78] B.D. Page, G.M. Lacroix, On-line steam distillation/purge and trap analysis of halogenated, nonpolar, volatile contaminants in foods, J AOAC Int, 78 (1995) 1416-1428.

[79] M. Lis-Balchin, G. Buchbauer, K. Ribisch, M.T. Wenger, Comparative antibacterial effects of novel Pelargonium essential oils and solvent extracts, Lett Appl Microbiol, 27 (1998) 135-141.

[80] I. Hinneburg, R.H. Neubert, Influence of extraction parameters on the phytochemical characteristics of extracts from buckwheat (Fagopyrum esculentum) herb, J Agric Food Chem, 53 (2005) 3-7.

[81] H.B. Xiao, M. Krucker, K. Albert, X.M. Liang, Determination and identification of isoflavonoids in Radix astragali by matrix solid-phase dispersion extraction and high-performance liquid chromatography with photodiode array and mass spectrometric detection, J Chromatogr A,

1032 (2004) 117-124.

[82] M.W. Biavatti, C.A. Koerich, C.H. Henck, E. Zucatelli, F.H. Martineli, T.B. Bresolin, S.N. Leite, Coumarin content and physicochemical profile of Mikania laevigata extracts, Z Naturforsch C, 59 (2004) 197-200.

[83] C.D. Bevan, P.S. Marshall, The use of supercritical fluids in the isolation of natural products, Nat Prod Rep, 11 (1994) 451-466.

[84] M. Adam, M. Juklova, T. Bajer, A. Eisner, K. Ventura, Comparison of three different solid-phase microextraction fibres for analysis of essential oils in yacon (Smallanthus sonchifolius) leaves, J Chromatogr A, 1084 (2005) 2-6.

[85] C. Bicchi, C. Cordero, E. Liberto, B. Sgorbini, P. Rubiolo, Reliability of fibres in solid-phase microextraction for routine analysis of the headspace of aromatic and medicinal plants, J Chromatogr A, 1152 (2007) 138-149.

[86] C. Bicchi, S. Drigo, P. Rubiolo, Influence of fibre coating in headspace solid-phase microextraction-gas chromatographic analysis of aromatic and medicinal plants, J Chromatogr A, 892 (2000) 469-485.

[87] J. Paolini, J. Costa, A.F. Bernardini, Analysis of the essential oil from the roots of Eupatorium cannabinum subsp. corsicum (L.) by GC, GC-MS and 13C-NMR, Phytochem Anal, 18 (2007) 235-244.

[88] C. Deng, G. Song, Y. Hu, Application of HS-SPME and GC-MS to characterization of volatile compounds emitted from Osmanthus flowers, Ann Chim, 94 (2004) 921-927.

[89] E.M. Shin, H.Y. Zhou, G.H. Xu, S.H. Lee, I. Merfort, Y.S. Kim, Anti-inflammatory activity of hispidol A 25-methyl ether, a triterpenoid isolated from Ponciri Immaturus Fructus, Eur J Pharmacol, 627 (2010) 318-324.

[90] K.Y. Moon, B.S. Hahn, J. Lee, Y.S. Kim, A cell-based assay system for monitoring NF-kappaB activity in human HaCat transfectant cells, Anal Biochem, 292 (2001) 17-21.

[91] J.K. Srivastava, M. Pandey, S. Gupta, chamomile, a novel and selective COX-2 inhibitor with anti-inflammatory activity, Life Sci, 85 (2009)

663-669.

[92] N. Bhaskaran, S. Shukla, J.K. Srivastava, S. Gupta, chamomile: an anti-inflammatory agent inhibits inducible nitric oxide synthase expression by blocking RelA/p65 activity, Int J Mol Med, 26 (2010) 935-940.

[93] J.K. Srivastava, S. Gupta, Antiproliferative and apoptotic effects of chamomile extract in various human cancer cells, J Agric Food Chem, 55 (2007) 9470-9478.

ABSTRACT IN KOREAN

국문 초록

국화과 식물 전체의 11%에 속하는 엉겅퀴아과의 대부분은 엉겅퀴류 식물로 총 83 속, 2500 여 종이 전세계에 분포하며, 이 중 국내에는 10 여 종이 자라고 있는 것으로 확인된다. 가장 일반적으로 알려져 있는 엉겅퀴(*Cirsium japonicum*)의 한약재명은 대계, 영문명은 Milk thistle 로 예로부터 지혈작용, 이뇨제, 소염제, 독소 배출 효과에 사용되고 있다. 또한, 지느러미 엉겅퀴(*Carduus crispus*)는 한방에서 비렴이라는 이름을 가지며, 영문명 welted thistle 로 전초를 주로 관절염, 감기, 간염, 소변출혈, 요로감염 등에 사용하고, 종기와 치질 환부에 직접 바르면 효과가 좋은 것으로 알려져 있다. 지느러미 엉겅퀴는 현재 직접적으로 한약재나 민간요법으로 많이 사용되는 식물은 아니기 때문에 관련 연구가 거의 진행되어 있지 않지만, 예로부터 관절염, 간염 또는 바이러스 등에 효과가 있는 것으로 알려져 있어 이를 바탕으로 항암, 항염증, 항비만 효과를 확인해 보았다. 그 결과 가장 높은 효과가 나타난 항비만 활성에 대한 효능 물질을 탐색하고자 본 연구를 진행하였다. 지느러미 엉겅퀴의 메탄올 추출물이 분화된 3T3-L1 세포의 지방 축적을 억제하는 효과가 있는 것을 확인하였고, 이와 관련된 활성

물질을 찾기 위해 EA 분획물(CE), high speed counter-current chromatography (HSCCC) 장치를 사용하여 elution extrusion counter-current chromatography (EECCC) 방법으로 추가 분리한 5 개의 분획물과 2 개의 단일 성분(Kaempferol-rhamnoside 와 apigenin), 이 중 6 번째 분획물로 얻어진 apigenin 의 순으로 지방 축적 억제 효과와 지방 생성에 관여하는 주요 전사 인자인 PPARγ 와 C/EBPα 의 단백질 발현을 억제 효과를 확인하였다. Apigenin 은 지방산의 산화와 당흡수를 촉진하여 미토콘드리아 내 ATP 생산을 증가시키는 AMPK 의 인산화 역시 활성화시키는 것을 확인할 수 있었다. 또한, 분화 8 ~ 9 일째 불규칙적으로 세포가 파괴되는 morphology 가 관찰되어, 이를 바탕으로 apigenin 이 caspase-3 의 active form 을 활성화시키는 것을 확인하여 *Carduus Crispus* 의 apigenin 이 분화된 3T3-L1 세포에서 세포사멸을 유도하는 방법으로 지방 세포를 사멸시키는 것으로 최종 판단하였다. 추가적으로 다른 엉겅퀴류의 대표적인 식물인 *Cirsium japonicum* 에서 분리된 지표 물질 중 pectolinarin 성분이 농도 의존적으로 분화된 3T3-L1 세포의 지방 축적을 감소시키는 것을 확인하였으며, 이것이 스테롤 조절 요소인 SREBP-1 를 억제하면서 AMPK 활성화를 통한 지방 생성 억제 효과임을 확인하였다. 또한, 세포 내에서 ROS 생성과 heme oxygenase (HO)-1 발현을 억제하는 결과를 토대로 pectolinarin 은 3T3-L1 adipocyte 에서 지방 산화 효과(fat oxidation effect)를 나타내는

것으로 판단할 수 있었다. 본 연구 결과를 바탕으로 *Carduus Crispus* 의 지방 축적 억제 효과는 apigenin 이 분화된 3T3-L1 세포에서 세포사멸을 유도하는 과정이 주된 요인으로 판단되었고, 추가적으로 비교해 본 *Cirsium japonicum* 의 pectolinarin 은 이와 달리 지방 산화 효과(fat oxidation effect)를 가지는 것으로 결론낼 수 있었다.

국화과 식물인 캐모마일(*Matricaria recutita*)은 원산지가 영국이나 현재는 전 세계에서 찾아볼 수 있고, 캐모마일의 방향유는 긴장 완화, 두통 등의 통증 완화와 몸을 따뜻하게 해주는 효과도 갖고 있으며, 차로 마시면 위장 장애의 완화에 도움을 주는 것으로 알려져 있다. 저먼 캐모마일에서 항암, 항염증, 항비만 활성을 탐색한 결과, 항염증 효과가 가장 뛰어난 것으로 확인하였다. 캐모마일의 항염증 효과는 이미 보고된 바가 있지만, 그 활성 성분을 탐색한 연구는 진행되지 않아 저먼 캐모마일의 항염증 활성을 나타내는 주요 활성 성분을 확인하고자 본 연구를 진행하였다. 캐모마일 메탄올 추출물은 RAW 264.7 macrophage에서 염증 반응 생성물인 Nitric oxide (NO)와 염증 반응에 관여하는 NF-κB 생성을 가장 높게 억제하였다. 극성이 낮은 메탄올 추출물은 방향성을 가진 정유 성분을 많이 함유하기 때문에 본 연구에서는 캐모마일 메탄올 추출물의 정유 성분을 분석할 필요를 가졌으나, 캐모마일은 휘발성 성분이 전체의 0.4% 정도로 매우 미미하여 추출이 어렵고, 수급 방법도 없었기 때문에, 비

록 분석을 위한 추출 방법이지만 HS-SPME (Head space-solid phase microextraction) / GC-MS (gas chromatography-mass spectrometry) 방법을 활용하여 캐모마일의 정유 성분 분석을 시도하였다. 캐모마일 건초 시료에서 6가지 주요 정유 성분인 β-farnesene, spathulenol, caryophyllene oxide, α-bisabolol oxide B, α-bisabolol, chamazulene을 바탕으로 추출 시간, 추출 온도, GC-MS에서 시료를 탈착하는 시간을 각각 달리하여 추출된 함량을 비교 분석하였고, 최종적으로 추출물 0.5 g, 추출 시간 30분, 추출 온도 100°C, 탈착 시간 5분이 가장 최적화된 방법임을 확인하였다. 이 방법으로 주요 성분을 포함하여 알려져 있는 총 105개의 캐모마일 정유 성분 중 41개를 확인하였고, 동일한 방법으로 캐모마일의 물 100% 추출물, 메탄올 100% 추출물과 캐모마일 메탄올 추출물의 헥산 분획물에 함유되어 있는 정유 성분을 GC-MS에서 비교, 분석하였다. 캐모마일의 물 추출물은 건초 시료에서 확인된 정유 성분 중 비중이 큰 α-bisabolol oxide B를 소량 함유하였으며, β-farnesene, trans-nerolidol, spathulenol, chamazulene은 확인되지 않았다. 가장 많은 함량을 차지한 화합물은 herniarin이었으며, 그 외 건초나 유기 용매 추출물에서는 확인되지 않았던 cocoa hexenal, tetraglyme 등이 검출되었으나, 유기 용매 추출물보다 정유 성분의 종류와 양이 모두 현저히 낮게 나타났다. 반면 유기 용매 추출물은 건초 시료의 결과와 유사하게 α-bisabolol oxide B, β-farnesene, 2-(2,4-Hexadiynylidene)-1,6-dioxaspiro(4,4)non-3-ene을 다량으로 함유하

고 있었으며, 헥산 분획물에서 확인된 물질은 메탄올 추출물에서 확인했던 휘발성 정유 성분과 유사하게 나타났다. 이로써 메탄올 추출물이 항염증 활성을 가지는 α-bisabolol oxide B, β-farnesene 등의 성분을 다량 포함하기 때문에 효과가 높게 나타난 것으로 판단되었다. 캐모마일의 활성 물질의 탐색을 위해 정유 성분 외에 비휘발성 성분의 활성으로 NO와 NF-κB의 억제 효과를 따라 탐색적 분리 실험을 시행하였다. 캐모마일 메탄올 추출물은 EA 분획물, silica gel column chromatography를 통하여 분리된 7개의 분획물, 이 중 높은 효과와 독성을 보이지 않은 5번째 분획물을 추가적으로 Diaion HP-20 column chromatography를 통하여 분획하였고, 이 과정에서 얻은 총 5개의 분획물 중 dicaffeoyl quinic acids (50% MeOH, DCQ), apigenin 7-O-glucoside 유도체 (70% MeOH, A7G), tetracoumaroyl thermospermine (90% MeOH, TCTS)의 3가지 주요 성분을 다량 함유한 enriched fractions가 분리되었다. 이 중 TCTS enriched fraction에서 가장 높은 NO 생성 억제 효과 및 iNOS와 COX 단백질 발현 억제 효과를 나타내었으며, 특히 COX-1 단백질 발현에 영향을 주지 않는 반면, COX-2 단백질 발현만 억제하는 것을 확인하였다. TCTS의 항염증 기전을 확인하는 단계에서 ERK/Akt/STAT3의 경로를 통하여 효과를 나타내는 것을 확인할 수 있었다. 본 연구에서는 캐모마일 메탄올 추출물의 항염증 활성에 대한 주요 활성 성분 탐색을 통하여 정유 성분으로 α-bisabolol oxide B와 β-farnesene을 확인하였고, 비휘발성 물질로는

TCTS가 ERK/Akt와 STAT3의 억제를 통해 항염증 효과를 나타내며, 특히 COX-1에 영향을 주지 않고, COX-2를 억제하는 것을 확인할 수 있었다.

Keywords: *Carduus crispus* L., *Matricaria recutita*, anti-adipogenic activity, anti-inflammatory activity, apigenin, pectolinarin, tetracoumaroyl thermospermine

학번: 2009-30474